AD-A141 597 DYNAMICAL PROPERTIES OF DISORDERED SYSTEMS(U) 1/1
CALIFORNIA UNIV LOS ANGELES DEPT OF PHYSICS
R L ORBACH ET AL. 21 MAY 84 N00014-75-C-0245

UNCLASSIFIED F/G 12/1 NL

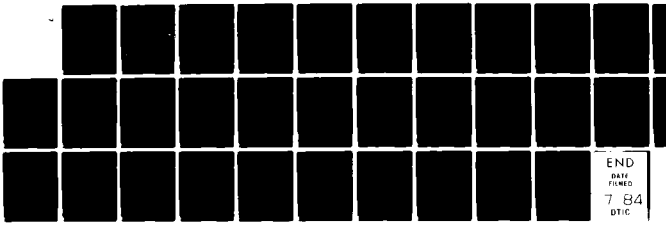

END
DATE FILMED
7 84
DTIC

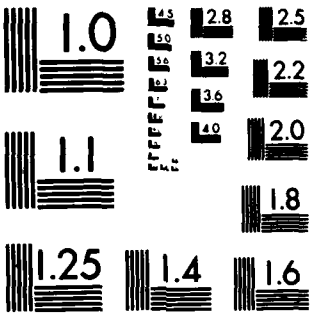

FINAL REPORT

Office of Naval Research Contract No. N00014-75-C-0245

DYNAMICAL PROPERTIES OF DISORDERED SYSTEMS

Physics Department
University of California
Los Angeles, California 90024

Submitted by the principal investigator:

Raymond Orbach

Raymond L. Orbach
(213) 825-4281

Charles Kennel
Chairman, Department of Physics

Ann Cinderella
Contracts and Grants Officer

Submitted May 21, 1984

I. Introduction

This final report covers the most recent period of the Office of Naval Research Contract No. N00014-75-C-0245, titled "DYNAMICAL PROPERTIES OF DISORDERED SYSTEMS". During this period, research has been completed on a variety of research problems contained in ONR Research Proposal. The principal areas of research can be summarized under the following categories:

1) The fractal interpretation of amorphous structures
2) Non-linear conductivity of low dimensional materials
3) The effect of anodization on the superconducting transition temperature
4) The time dependence of the remanent magnetization of spin glasses
5) The experimental opportunities for physics at high magnetic fields

In the next Section, we outline the research accomplishments in each of these areas. The detailed references to published research supported in these areas by the Office of Naval Research is contained in Section III.

II. Research accomplishments

1) The fractal interpretation of amorphous structures

During the period 1982-83, we began an intensive investigation of the dynamical properties of physical systems which were fractal in geometry. We showed that the density of states on a fractal can be calculated by taking into account the scaling properties of both the volume and the connectivity. We used a Green's function method developed elsewhere, utlizing a relationship to the diffusion problem. We found that proper mode counting required a reciprocal space with a new intrinsic fracton dimensionality $\tilde{d} = 2\bar{d}/(2 + \theta)$. Here, $\bar{d}$ is the effective dimensionality, and θ the exponent giving the dependence of the diffusion constant on distance. For example, we find for percolation clusters $\bar{d} = 4/3$ within the numerical accuracy available, independent of Euclidean dimensionality d. Crossover to normal behavior at low frequencies was discussed for finite fractals and for percolation above the percolation threshold p_c. Relevance to experimental results on proteins was also discussed.

In a follow-up piece of research, we calculated the density of states for lattice vibrations on a fractal with careful attention paid to the normalization condition. It was found that at the cross-over between Debye-type excitations (long wavelength) and "fracton" excitations (short length scale) the density of states is discontinuous. The size of the discontinuity was related to the ratio of the fracton dimensionality to the Euclidean dimensionality. An application was made to percolating structures. A set of missing modes was identified which may be the origin of the two-level systems hypothesized for amorphous structures. The specific heat of epoxy-resin exhibits a cross-over from a Debye-type region (T<8K) to a region (8-50K) where the vibrational density of states depends linearly on the frequency. Over the same frequency regime, the thermal conductivity exhibits an effective phonon mean free path of the order of (or less then) a lattice constant. We interpreted this behavior in terms of quantized fractons, with an energy range 8-50K, and we suggested that these fracton states are localized. This was consistent with the usual interpretation of a precipitous drop in the phonon mean free path at the cross-over energy of 8K. Analogous behavior was argued for the thermal properties of glasses which exhibit a similar structure in the thermal conductivity. Recent neutron-irradiated quartz experiments tend to confirm this interpretation.

2) Non-linear conductivity of low dimensional materials

The frequency dependence of the electrical conductivity was examined for a classical hopping model of a random one-dimensional system in the presence of a superposed static electric field. The effect of the field was taken as a constant bias for the left-right jump rates. A general expression was derived for the mean velocity and frequency-dependent conductivity. Explicit evaluation of these equations was given for correlated and uncorrelated hopping rates: (1) in general for high frequencies and (2) to lowest order in the disorder for all frequencies. In the latter case, an initial decrease in the frequency dependent conductivity for very small frequencies was found, with the real part of the conductivity varying as the square of the frequency while the imaginary pary varyied as the cube of the frequency. For larger frequencies, the conductivity crossed over to the form previously calculated by Alexander and Orbach (proportional to the square root of the frequency). The cross-over frequency increases with the bias. In addition, the variance in the autocorrelation function was calculated in the long-time limit, for weak disorder in the symmetric case. It was shown that fluctuations do not significantly affect the determination of this quantity under these conditions.

3) The effect of anodization on the superconducting transition temperature

We measured the superconducting transition temperature of anodized aluminum films of grain sizes ranging from less than 100 to 3,000 angstroms. The transition temperature is 1.8K for films of grain size 100 angstroms, and decreased monotonically with increasing grain size to 1.2K for 3,000 angstrom grains. The effect depended only on the volume of the grains. We concluded that the phonon softening model appeared to break down for thin aluminum grains.

4) The time dependence of the remanent magnetization of spin glasses

The time decay of the thermoremanent magnetization (M_{TRM}) was measured in 1.0% Cu:Mn and 2.6% Ag:Mn spin-glasses. It was shown that M_{TRM} was neither an algebraic nor a logarithmic function of time. Instead, it was found that M_{TRM} can be characterized by a "streched" exponential: $M_{TRM} = M_0 \exp[-C(t/t_0)^{1-n}/(1-n)]$. The prefactor ($M_0$) and the time-stretch exponent (n) are temperature dependent, whereas the exponential factor (C) and the relaxation rate ($1/t_0$) can be chosen to be independent of temperature throughout the spin glass region. In addition, we found M_0 to depend linearly on the cooling field H, whereas n, C, and $1/t_0$ are independent of H for H less than 30 Oersteds. Similar time dependences appear in the disorder-diffusion theory of Grassberger and Procaccia and the cooperative-relaxation theory of Ngai, but neither theory in its present form was found to be directly applicable to spin glasses.

5) The experimental opportunities for physics at high magnetic fields

A brief list of current areas of research in high magnetic field physics was investigated. Three distinct areas were examined in detail: (1) density of states for vibrational states on fractals ("fractons"), (2) the thermodynamic properties of exchange enhanced quasi-magnetic systems, and (3) p-state pairing in thin film or layered superconductors.

III. References to published work (numbering in accord with Section II)

1) "Density of states on fractals: 'fractons'", by S. Alexander and R. Orbach, Journal de Physique (Paris) Lettres 43, L-625 (1982).

"Fracton interpretation of vibrational properties of cross-linked polymers, glasses, and irradiated quartz", by S. Alexander, C. Laermans, R. Orbach, and H. M. Rosenberg, Phys. Rev. B28, 4615 (1983).

2) "Frequency dependence of the conductivity in presence of an electric field in one dimension: Weak disorder limit", by B. Derrida and R. Orbach, Phys. Rev. B27, 4694 (1983).

3) "Superconducting transition temperature in anodized aluminum", by C. Leemann, J. H. Elliott, G. Deutscher, R. Orbach, and S. A. Wolf, Phys. Rev. B28, 1644 (1983).

4) "Time decay of the remanent magnetization in spin-glasses", by R. V. Chamberlin, George Mozurkewich, and R. Orbach, Phys. Rev. Lett. 52, 867 (1984).

5) "On the physics of high magnetic fields", R. Orbach, in High Field Magnetism, ed. by M. Date (North Holland Publishing Company, Amsterdam, 1983), p. 3.

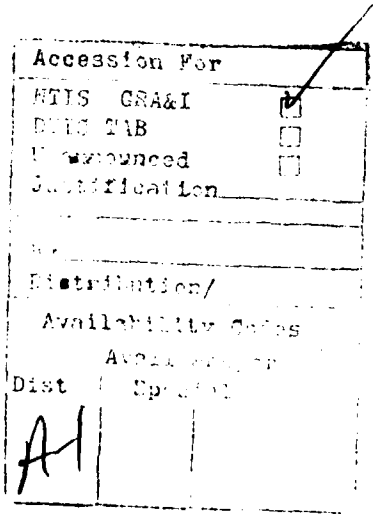

INSTRUCTIONS TO CONTRACTOR

This form *(in triplicate)* is for use in submitting **INTERIM** and **FINAL** reports to the Contracting Officer.

An **INTERIM** report is due at least every 12 months from the date of the contract and shall include (a) a listing of Subject Inventions during the reporting period, (b) a certification of compliance with required invention identification and disclosure procedures, and (c) any required information on Subcontracts having a Patent Rights clause awarded during the reporting period which has not been previously reported.

A **FINAL** report is due within 3 months after completion of the contract work and shall include (a) a listing of all Subject Inventions required by the contract to be reported, and (b) any required information on Subcontracts awarded having a Patent Rights clause which has not been previously reported.

U S GOVERNMENT PRINTING OFFICE 1976— 703-069/3088 2-1

Tome 43 N° 17 1er SEPTEMBRE 1982

LE JOURNAL DE PHYSIQUE - LETTRES

J. Physique — LETTRES **43** (1982) L-625 - L-631 1er SEPTEMBRE **1982**, PAGE L-625

Classification
Physics Abstracts
63.50 — 66.30

Density of states on fractals : « fractons »

S. Alexander

The Racah Institute, The Hebrew University, Jerusalem, Israel

and R. Orbach (*)

Ecole Supérieure de Physique et de Chimie Industrielles de la Ville de Paris,
10, rue Vauquelin, 75231 Paris Cedex 05, France

(*Reçu le 22 avril 1982, accepté le 7 juillet 1982*)

Résumé. — Nous calculons la densité d'états sur un fractal en tenant compte des propriétés d'échelles pour le volume et la connectivité. Nous utilisons la méthode de Green développée par ailleurs, qui utilise une relation au problème de diffusion. Nous avons trouvé que, pour compter les modes correctement, on doit avoir un espace réciproque avec une nouvelle dimensionnalité de fracton

$$\bar{\bar{d}} = 2\,\bar{d}/(2 + \bar{\delta})\,.$$

Ici, $\bar{d}$ est la dimension effective, et $\bar{\delta}$ est l'exposant que caractérise la variation de la constante de diffusion avec la distance. Par exemple, nous trouvons pour les amas de percolation, $\bar{\bar{d}} = 4/3$, quelle que soit la dimensionnalité Euclidienne d à la précision numérique disponible. Nous discutons le « crossover » vers un comportement normal aux basses fréquences pour des fractals finis, et pour la percolation au-dessus du seuil de percolation p_c. Nous examinons aussi la pertinence de nos prédictions en les confrontant à des résultats expérimentaux sur les protéines.

Abstract. — The density of states on a fractal is calculated taking into account the scaling properties of both the volume and the connectivity. We use a Green's function method developed elsewhere which utilizes a relationship to the diffusion problem. It is found that proper mode counting requires a reciprocal space with new intrinsic fracton dimensionality $\bar{\bar{d}} = 2\,\bar{d}/(2 + \bar{\delta})$. Here, $\bar{d}$ is the effective dimensionality, and $\bar{\delta}$ the exponent giving the dependence of the diffusion constant on distance. For example, we find for percolation clusters $\bar{\bar{d}} = 4/3$ within the numerical accuracy available, independent of the Euclidean dimensionality d. Crossover to normal behaviour at low frequencies is discussed for finite fractals and for percolation above the percolation threshold p_c. Relevance to experimental results on proteins is also discussed.

(*) Permanent address : Department of Physics, University of California, Los Angeles, California, 90024, U.S.A.

The purpose of this note is to calculate the density of states on fractals. We do this using a Green's function technique [1], which avoids the use of boundary conditions and wave vector counting. We show that the usual relationship between the density of states and the Euclidean dimensionality (d) does not apply. The density of states cannot be described in terms of an anomalous dimensionality ($\bar{d}$) alone but requires an additional index describing the internal structure. We determine a fracton dimensionality ($\bar{\bar{d}}$) of the relevant reciprocal space which assures proper mode counting for a fractal in terms of the index governing diffusion ($\bar{\delta}$) and the anomalous or fractal dimension ($\bar{d}$). The density of states for free particles and for lattice vibrations is determined. We apply these results to polymer chains, the triangular Sierpinski gasket, and to percolation networks.

We were directly motivated by the recent work of Stapleton *et al.* [2] who found an anomalous temperature dependence for the ESR spin-lattice relaxation time of iron in several proteins. They interpreted their measurements in terms of an anomalous vibrational density of states arising from a suggested fractal structure for the proteins. However, they included only the anomalous dimensionality $\bar{d}$ in their analysis.

The density of states on fractals should also be of interest in other situations. Examples would be the role of geometrical disorder in amorphous systems, and the specific heat of fractal-like systems in the intermediate temperature range (see below).

1. **Method of calculation.** — We consider problems defined on a fractal so that both the available volume and the connectivity are determined by the fractal geometry. An explicit way of realizing a fractal model is to consider solutions of the relevant equations on a network of wires connected in a suitable geometry [3]. We take the network to be homogeneous. Our results will apply for times or frequencies such that the associated distances are much larger than the size of the individual bonds making up the network, but much smaller than the total size of the network. Formally, we are assuming that one can define some local geometry on the fractal in which the Laplacian has its usual form (i.e. is equivalent to a local q^2 expansion). This is defined by the wires for a network model. While this may not be possible for all conceivable fractals, we believe it is certainly possible for most cases in which one would be interested. One finds that the formal relationship between problems initially described by Laplacians (or by equivalent finite difference equations [4]) is maintained.

The structure of the diffusion equation is such that it can be mapped onto a master equation, which in turn has the same form as the free particle Schrödinger equation and the equation of motion for mechanical vibrations (see Sec. 3 of Ref. [3], and Ref. [5]). This will enable us to map the eigenvalue density of states for the quantum vibrational problem onto the eigenvalue density of states of the diffusion problem. The latter can be obtained from the single site Green's function for the diffusion problem [1] :

$$N(\varepsilon) = -\frac{1}{\pi} \operatorname{Im} \langle \tilde{P}_0(-\varepsilon + i0^+) \rangle \tag{1}$$

where $\tilde{P}_0(\varepsilon)$ is the Laplace transform of $P_0(t)$, the autocorrelation function, with ε the spectral parameter. In physical terms, if a particle is initially at the origin at time $t = 0$, the probability of finding it there at time t is given by $P_0(t)$. We now calculate this quantity directly.

On a fractal one expects, in general, anomalous diffusion [6]. We write,

$$\langle r^2(t) \rangle \propto t^{2/(2+\bar{\delta})}, \tag{2}$$

where $\bar{\delta}$ is an index which depends on the geometry (i.e. it is the diffusion constant scaling exponent). In general, one expects $\bar{\delta} \neq 0$. The total volume available on the fractal, within the diffusion distance, is

$$V(t) \propto \langle r^2(t) \rangle^{\bar{d}/2}, \tag{3}$$

where $\bar{d}$ is the anomalous or fractal dimensionality. Thus,

$$\langle P_0(t) \rangle \propto [V(t)]^{-1} \propto t^{-\bar{d}/(2+\bar{\delta})}. \tag{4}$$

We have thus assumed that the diffusion length is given by a power law (Eq. (2)) and that it is the only relevant length scale in the problem. Using equation (1), one is immediately led to the eigenvalue density of states for the diffusion problem :

$$N(\varepsilon) \propto \varepsilon^x, \tag{5}$$

where

$$x = [\bar{d}/(2 + \bar{\delta})] - 1. \tag{6}$$

As shown explicitly in reference [1], the spectral parameter ε can be related to the energy eigenvalues of the vibrational problem by replacing ε by ω^2 and multiplying by ω :

$$N(\omega) \propto \omega^p, \tag{7}$$

where

$$p = 2x + 1 = [2\bar{d}/(2 + \bar{\delta})] - 1. \tag{8}$$

We refer to the quantized vibrational states on a fractal as fractons.

For positive $\bar{\delta}$, x and p are always smaller than the anomalous dimension result ($x = (\bar{d}/2) - 1$, $p = \bar{d} - 1$, as suggested in Ref. [2]). The reason for the difference is that the scale dependence of the elastic constants is also anomalous (i.e. it depends on $\bar{\delta}$). It is not sufficient to consider only the mass scaling described by $\bar{d}$.

Our results, equations (5)-(8), can be described by a « mode counting » reciprocal space of effective dimensionality

$$\bar{\bar{d}} = 2\bar{d}/(2 + \bar{\delta}). \tag{9}$$

We shall call this the fracton dimensionality. For a standard Laplacian ($\Delta \to q^2$) expansion, this is the relevant dimensionality. It determines the relevant Hilbert space for Laplacian equations on the fractal. We emphasize that the fracton dimensionality ($\bar{\bar{d}}$) is an intrinsic property of the fractal geometry. It differs from the mass scaling exponent, or the fractal dimensionality ($\bar{d}$), and from the diffusion constant scaling exponent ($\bar{\delta}$), in being independent of the manner in which the fractal is embedded in an external space (of Euclidean dimension d). The d dependence of $\bar{d}$ and $\bar{\delta}$ cancels out in equation (9).

We note that this seems to be the natural extension of a gradient expansion to fractals. The obvious alternative of expanding in undistorted real space gradients leads to a singular expansion ($\varepsilon \sim q^{2+\bar{\delta}}$) and a reciprocal space of dimensionality $\bar{d}$ (using Eq. (2)).

2. **Some examples.** — It is useful to consider some examples.

a) Consider a one dimensional chain whose configuration is described by a random walk or self-avoiding walk. One has

$$N^{\nu} \propto r, \tag{10}$$

where N is the length (number of units) of the chain. Thus,

$$\bar{d} = \nu^{-1}. \tag{11}$$

For diffusion *along* the chain,

$$N^2(t) \propto t,$$

and from equations (10) and (11),

$$\langle r^2(t) \rangle \propto \langle N^{2\nu}(t) \rangle \propto t^{\nu}, \tag{12}$$

so that

$$\bar{\delta} = 2(\bar{d} - 1), \tag{13}$$

leading to (Eqs. (6), (8), and (9)),

$$x = 1/2, \quad p = 0, \quad \text{and} \quad \bar{\bar{d}} = 1. \tag{14}$$

The fracton dimension ($\bar{\bar{d}}$) for this problem is identically one, and is independent of ν.

b) Consider a triangular ($d = 2$) Sierpinski gasket. One has [3, 7]

$$\bar{\delta} = [(\ln 5)/(\ln 2)] - 2 \approx 0.322, \tag{15a}$$

$$\bar{d} = (\ln 3)/(\ln 2) \approx 1.585, \tag{15b}$$

but the fracton dimension is (Eq. (9)),

$$\bar{\bar{d}} = 2(\ln 3)/(\ln 5) \approx 1.365. \tag{16}$$

Thus, the gasket is somehow more one dimensional than suggested by $\bar{d}$. For the eigenvalue density of states, one has the spectral parameter exponent (Eq. (6)),

$$x = [(\ln 3)/(\ln 5)] - 1 \approx -0.317, \tag{17a}$$

and the fracton ω exponent (Eq. (8)),

$$p = [2(\ln 3)/(\ln 5)] - 1 \approx 1.365. \tag{17b}$$

c) Consider a critical percolation network. Taking the infinite cluster at the critical percolation concentration p_c, one has from straight forward scaling considerations [8],

$$\bar{d} = d - (\beta/\nu), \tag{18}$$

where d is the Euclidean dimensionality of the external space, and [3, 6]

$$\bar{\delta} = (t - \beta)/\nu, \tag{19}$$

where t is the conductivity exponent. Thus,

$$\bar{\bar{d}} = 2(d\nu - \beta)/(t - \beta + 2\nu). \tag{20}$$

Table I. — *The fracton dimensionality* $\bar{\bar{d}}$ *defined in equation* (9) *and the eigenvalue density of states indices* x (*Eq.* (6)) *and* p (*Eq.* (8)) *as a function of the Euclidean dimensionality of the percolation problem* (d). *The fractal dimensionality* $\bar{d}$ (*Eq.* (18)) *and* $\bar{\delta}$ (*Eq.* (19)) *were computed from the numerical values in reference*[8].

d	$\bar{\bar{d}}$	x	p	$\bar{d}$	$\bar{\delta}$
2	1.36	− 0.32	0.36	1.9	0.80
3	1.42	− 0.29	0.42	2.5	1.55
4	1.39	− 0.30	0.39	3.3	2.71
5	1.44	− 0.28	0.44	3.8	3.3
∞	4/3	− 1/3	1/3	4	4

We give results for $\bar{\bar{d}}$ in table I as a function of the Euclidean dimensionality (d) for Stauffer's values [8] of the indices t, β, and ν for the percolation problem. One notes the very weak dependence of the fracton dimensionality ($\bar{\bar{d}}$) on the Euclidean dimensionality (d) of the percolation problem. This is in sharp contrast to the behaviour of $\bar{d}$ and $\bar{\delta}$. The table certainly suggests the conjecture that, for percolation on the infinite cluster,

$$\bar{\bar{d}} = 4/3 , \tag{21}$$

independent of d (see note added in proof).

3. **Crossover and finite size effects.** — The Laplace transform of equation (2) yields a relation between length scale and the Laplace transform spectral parameter ε. We are able to find a characteristic diffusion length scale appropriate to the spectral parameter ε, λ_ε, which varies as [3]

$$\lambda_\varepsilon \propto \varepsilon^{-1/(2+\bar{\delta})} . \tag{22a}$$

Mapping onto the vibrational problem as before,

$$\lambda_\omega \propto \omega^{-2/(2+\bar{\delta})} . \tag{22b}$$

Fractal behaviour is found for length scales less than the size (L) of a fractal object. For larger length scales, the solutions are, in essence, uniform over the fractal and the density of states is determined by the boundary conditions. Crossover to fractal behaviour occurs when $\lambda_\varepsilon \lesssim L$, or for energies

$$\varepsilon_{\text{c.o.}} \approx \omega_{\text{c.o.}}^2 \gtrsim L^{-(2+\bar{\delta})} , \tag{23}$$

where the subscript c.o. means crossover. For $\varepsilon > \varepsilon_{\text{c.o.}}$ (or $\omega > \omega_{\text{c.o.}}$), the eigenvalue density of states is then given by equation (5) (or Eq. (7)). For a percolation network above p_c, one predicts normal d-dimensional low frequency vibrational density of states ($p = d - 1$) crossing over to fracton behaviour for vibrational frequencies above (Eq. (23))

$$\omega_{\text{c.o.}}(p) \propto \xi_p^{-(2+\bar{\delta})/2} \tag{24}$$

where ξ_p is the percolation correlation length.

4. **Discussion.** — We conclude with some remarks concerning the relevance of our results to experiment. We have analysed the eigenvalue density of states for diffusion on a fractal geometry, and mapped our results onto the vibrational eigenvalue density of states for systems with the same geometrical structure. For the vibration problem, this assumes that both the elastic constants and the inertial mass are appropriate to a free fractal. It is important to emphasize that this is not necessarily a proper physical description. It is, in fact, hard to think of a situation where the vibration spectrum of a polymer would be adequately described by our free fracton model. For gels, the mass density is always dominated by the solvent, and therefore scales with the Euclidean dimensionality of the external space (d). Any fractal anomalies would only reflect the scaling properties of the elastic constants. It is conceivable that something similar occurs for proteins where one would also expect an essentially uniform density. This might be relevant to the interpretation of the results of Stapleton *et al.* [2] and to other measurements in which the vibrational density of states of proteins is important [9].

This work was supported in part by the U.S. National Science Foundation and the U.S.

Office of Naval Research. We wish to acknowledge helpful correspondence with H. J. Stapleton, and very useful conversations with T. C. Lubensky, R. Rammal, G. Toulouse, and J. Vannimenus (see note added in proof).

Note added in proof. — Professor T. C. Lubensky has noted (private communication) that some intriguing consequences follow if one takes seriously the results of the table for the percolation problem. He notes that if one assumes that $\bar{\bar{d}} = 4/3$, independent of d, one can use equation (20) to generate an expression for the exponent t in terms of ν and β :

$$t = (1/2)\,[\nu(3\,d - 4) - \beta]\,.$$

Two consequences are worth noting.

1) Using the values of β and ν following from the den Nijs conjecture at $d=2$ (M. P. M. den Nijs, *Physica* (Utrecht) **A 95** (1979) 449) : $\beta = 5/36$ and $\nu = 4/3$, one finds $t = 91/72 = 1.264$. This differs from $t \cong 1.1$ presented by S. Kirkpatrick (*La matière mal condensée*, Ed. by R. Balian, R. Maynard and G. Toulouse (North-Holland publishing company, Amsterdam) 1979, p. 321), and is not in accord with the relation $t = \nu$ (A. K. Sarychev and A. P. Vinogradoff, *J. Phys.* **C 14** (1981) L-487). A very recent finite size scaling (simulations on finite size strips) of B. Derrida and J. Vannimenus (submitted for publication, 1982) finds $t \cong 1.28$, in close accord with the above consequence ($t = 1.264$) of setting $\bar{\bar{d}} = 4/3$.

2) The links and node model led A. S. Skal and B. I. Shklovskii [*Fiz. Tekh. Poluprov.* **8** (1974) 1582 (*Sov. Phys. : Semicond.* **8** (1975) 1029)] to define $t = (d - 2)\,\nu + \zeta$. Setting $\bar{\bar{d}} = 4/3$, solving for t, and using appropriate scaling relationships, leads to the expression, valid for all d,

$$\zeta = (1/2)\,(\beta + \gamma)\,.$$

G. S. Grest and M. J. Stephen (*Phys. Rev. Lett.* **38** (1977) 567) and C. Dasgupta, A. B. Harris and T. C. Lubensky (*Phys. Rev.* **B 17** (1978) 1375) show that $\zeta_{\text{pert}} = 1 + 0(\varepsilon^2)$ where $\varepsilon = 6 - d$. If we use perturbation theory results for β and γ (R. G. Priest and T. C. Lubensky, *Phys. Rev.* **B 13** (1976) 4159; **B 14** (1976) 5125; D. J. Amit, *J. Phys.* **A 9** (1976) 1441) :

$$\beta = 1 - (1/7)\,\varepsilon - (61/7^3\,3^2\,2^2)\,\varepsilon^2 + \cdots$$

$$\gamma = 1 + (1/7)\,\varepsilon + (565/7^3\,3^2\,2^2)\,\varepsilon^2 + \cdots$$

we find

$$\zeta_{\text{pert}} = 1 + \varepsilon^2/49$$

as required to $0(\varepsilon^2)$. For $d = 2$, $t_{\text{pert}} = \zeta = 1.33$, obviously outside the range of « safe » convergence ($\varepsilon = 4$), but remarkably close to the conjecture ($\bar{\bar{d}} = 4/3$) value of $t = 1.264$.

Finally, from another perspective, R. Rammal and Angles d'Aurioc (submitted for publication, 1982) have found values for $\bar{d}$ and $\bar{\delta}$ for the Sierpinski sponge in d dimensions. They find

$$\bar{d} = [\ln (d + 1)]/\ln 2\,, \qquad \bar{\delta} = \{[\ln (d + 3)]/\ln 2\} - 2$$

so that

$$\bar{\bar{d}} = 2[\ln (d + 1)]/\ln (d + 3)\,.$$

These results agree with ours for the case we considered, $d = 2$. In addition, the asymptotic $d \to \infty$ limit for $\bar{\bar{d}}$ is 2, quite different from the $d \to \infty$ limit for the percolation problem, 4/3. The ratio, $\bar{\bar{d}}/\bar{d} = (\ln 4)/[\ln (d + 3)]$ is always less than unity for $d \geqslant 2$, exhibiting the same trend as we have exhibited for $d = 2$.

References

[1] ALEXANDER, S., BERNASCONI, J., and ORBACH, R., *J. Physique Colloq.* **39** (1978) C6-706.
[2] STAPLETON, H. J., ALLEN, J. P., FLYNN, C. P., STINTON, D. G., and KURTZ, S. R., *Phys. Rev. Lett.* **45** (1980) 1456.
[3] ALEXANDER, S., preprint, submitted to *J. Low Temp. Phys.*, 1982.
[4] ALEXANDER, S., unpublished.
[5] ALEXANDER, S., BERNASCONI, J., SCHNEIDER, W., and ORBACH, R., *Rev. Mod. Phys.* **53** (1981) 175.
[6] GEFEN, Y., AHARONY, A., and ALEXANDER, S., to be submitted for publication, 1982.
[7] GEFEN, Y., AHARONY, A., MANDELBROT, B. B., and KIRKPATRICK, S., *Proc. Intern. Conf. on Disordered Systems and Localization* (Rome, 1981) ; *Phys. Rev. Lett.* **47** (1981) 1771.
[8] STAUFFER, D., *Phys. Rep.* **54** (1979) 1.
[9] COHEN, S. G., BAUMINGER, E. R., NOWIK, I., OFER, S., and YARIV, J., *Phys. Rev. Lett.* **46** (1981) 1244.

PHYSICAL REVIEW B VOLUME 28, NUMBER 8 15 OCTOBER 1983

Fracton interpretation of vibrational properties of cross-linked polymers, glasses, and irradiated quartz

S. Alexander,* C. Laermans,† R. Orbach,‡ and H.M. Rosenberg§
École Supérieure de Physique et Chimie Industrielles, 10 rue Vauquelin, F-75005 Paris, France
(Received 28 March 1983)

The density of states for thermal vibrations on a fractal is calculated with careful attention paid to the normalization condition. It is found that at the crossover between Debye-type excitations (long wavelength) and "fracton" excitations (short-length scale) the density of states is discontinuous. The size of the discontinuity is related to the ratio of the fracton dimensionality to the Euclidean dimensionality. Application is made to percolating structures. A set of missing modes is identified which may be the origin of the two-level systems hypothesized for amorphous structures. The specific heat of epoxy resin exhibits a crossover from a Debye-type region ($T < 8$ K) to a region (8–50 K) where the vibrational density of states depends linearly on the frequency. Over the same frequency regime, the thermal conductivity exhibits an effective phonon mean free path of the order of (or less than) a lattice constant. We interpret this behavior in terms of quantized fractons, with an energy range 8–50 K, and we suggest that these fracton states are localized. This is consistent with the usual interpretation of a precipitous drop in the phonon mean free path at the crossover energy of 8 K. Analogous behavior is argued for the thermal properties of glasses which exhibit a similar structure in the thermal conductivity. Recent neutron-irradiated quartz experiments tend to confirm this interpretation.

I. INTRODUCTION

Two of us have suggested that the concept of fractals[1] can be applied to the vibrational properties of macromolecules and have derived the vibrational density of states for fractal structures.[2] We found that the usual Debye-type density of states crosses over to a "fracton" density of states for length scales less than some characteristic length (L), corresponding to frequencies greater than a crossover frequency ω_{co}. We denote the Euclidean dimensionality by d, and call the density dimensionality of the fractal $\bar{d}$ (the so-called Hausdorff dimensionality). (Thus the mass increases with increasing length r as $r^{\bar{d}}$). The exponent giving the dependence of the diffusion constant on distance is denoted by θ, such that

$$D(r) \propto r^{-\theta} . \tag{1}$$

Alexander and Orbach[2] show that the density of vibrational states in the regime of fractal behavior can be written as

$$N(\omega) \propto \omega^{\tilde{d}-1} \tag{2}$$

where $\tilde{d}$ is the fracton dimensionality,

$$\tilde{d} = 2\bar{d}/(2+\theta) . \tag{3}$$

In Euclidean space, $N(\omega) \propto \omega^{d-1}$. The crossover frequency scales as

$$\omega_{co} \propto L^{-(2+\theta)/2} . \tag{4}$$

Recent experiments of Kelham and Rosenberg[3] suggest that experiments involving the heat capacity and thermal transport of epoxy resins may be exhibiting behavior relevant to the predictions of Ref. 2. We shall describe the relevance of these experiments to fractal behavior below, but first it is necessary to make explicit the crossover from phonon (long-length scales) to fracton (short-length scales) density of states. In particular, we need to derive the normalization coefficients which make the above Eqs. (1)–(4) quantitative.

II. PHONON AND FRACTON DENSITY OF STATES

We wish to normalize the long-wavelength phonon density of states to a volume L^d. This is because the phonon character of the elementary vibrational excitations terminates at the (minimum) length scale L. Thus we set

$$N_{ph}(\omega) = d(L/a)^d[(\omega)^{d-1}/(\omega_D)^d] , \tag{5}$$

where a is an atomic distance which sets the shortest length scale in the problem (i.e., fracton behavior is obtained for length scales on a descending basis between L and a). Thus

$$\omega_{co} = (a/L)\omega_D , \tag{6}$$

where ω_D is the apparent Debye frequency as projected by the low-frequency velocity of sound. The integral of Eq. (5) from 0 to ω_{co} equals unity, indicating that there is one mode per volume L^d as required. Thus at the crossover frequency one finds

$$N_{ph}(\omega_{co}) = d/\omega_{co} . \tag{7}$$

The fracton regime is a little more complex. From the definition of the Hausdorff dimensionality there will be $(L/a)^{\bar{d}}$ atoms per molecule. This leads to an appropriate

fracton density of states,[2]

$$N_{\rm fr}(\omega)=\bar{\bar{d}}(L/a)^{\bar{d}}[(\omega)^{\bar{\bar{d}}-1}/(\omega_{\rm FD})^{\bar{\bar{d}}}] . \tag{8}$$

We have introduced another quantity, the so-called fracton Debye frequency,

$$\omega_{\rm FD}=\omega_D(L/a)^{\theta/2} . \tag{9}$$

This quantity sets the upper limit on the frequency regime of fracton behavior. Indeed, if we integrate Eq. (8) from $\omega_{\rm co}$ to $\omega_{\rm FD}$ we find $(L/a)^{\bar{d}}-1$ modes as required. That is, there is one-phonon mode per volume L^d, and $(L/a)^{\bar{d}}-1$ fracton modes, so that in total one finds $(L/a)^{\bar{d}}$ modes per volume a^d. At the crossover frequency, Eq. (8) reduces to

$$N_{\rm fr}(\omega_{\rm co})=\bar{\bar{d}}/\omega_{\rm co} . \tag{10}$$

We therefore find the important relationship at crossover,

$$N_{\rm fr}(\omega_{\rm co})/N_{\rm ph}(\omega_{\rm co})=\bar{\bar{d}}/d . \tag{11}$$

Because we believe $\bar{\bar{d}}<d$, we shall discover that the experiment appears to be in conflict with the ratio (11), even though the remainder of the spectrum appears to be consistent with the ideas of fractal behavior (see *Note added in proof*).

III. APPLICATION TO PERCOLATION

Though the experimental portions of this paper are certainly not described by percolating networks, it is of interest (and possibly of experimental importance) to carry through the ideas of the previous section to illustrate an example of fractal structure. It is necessary, however, to distinguish between the infinite cluster and finite clusters when calculating the full density of vibrational states for percolating networks.

As shown in Ref. 2, one can use the concept of fractals for percolating structures, with $(L/a)^{\bar{d}}$ atoms (sites) per molecule, where L is the percolation correlation length ξ_p. Denoting the infinite cluster by the superscripts IC, we find Eq. (8) becomes

$$N_{\rm fr}^{\rm IC}(\omega)=\bar{\bar{d}}(L/a)^{\bar{d}}[(\omega)^{\bar{\bar{d}}-1}/(\omega_{\rm FD})^{\bar{\bar{d}}}] . \tag{12}$$

The finite clusters need to be considered because the (specific-heat) density of states will be the sum of the infinite and finite cluster density of states. The probability per site, or atom, of belonging to a cluster of size $R<L$ is

$$[P(R)]_{\rm FC}=(d-\bar{\bar{d}})(R/a)^{-(1+d-\bar{\bar{d}})} , \tag{13}$$

where the subscript FC means finite cluster. Equation (13) leads to

$$\int_a^L [P(R)]_{\rm FC}\,dR=1-(a/L)^{d-\bar{\bar{d}}} , \tag{14}$$

the probability of belonging to a finite cluster. By defining

$$R(\omega)/a=(\omega/\omega_{\rm FD})^{-2/2+\theta} , \tag{15}$$

only clusters with $R>R(\omega)$ contain modes of frequency ω. Next, the total number of sites (or atoms) in a volume L^d is, from Eq. (14),

$$(L/a)^d[1-(a/L)^{d-\bar{\bar{d}}}]_{\rm FC}+[(L/a)^{\bar{\bar{d}}}]_{\rm IC}=(L/a)^d , \tag{16}$$

and therefore not critical.

Equations (13) and (14) together enable us to calculate the total number of modes in the finite cluster. We have

$$\begin{aligned} N_{\rm fr}^{\rm FC}(\omega)&=(L/a)^d\int_{R(\omega)}^{L}(\bar{\bar{d}}/\omega)(\omega/\omega_{\rm FD})^{\bar{\bar{d}}}P(R)\,dR \\ &=L^d(\bar{\bar{d}}/\omega)(\omega/\omega_{\rm FD})^{\bar{\bar{d}}} \\ &\quad\times\{[a/R(\omega)]^{\bar{\bar{d}}-d}-(a/L)^{\bar{\bar{d}}-d}\} . \end{aligned} \tag{17}$$

Adding $N_{\rm fr}^{\rm IC}(\omega)$ from Eq. (12) to Eq. (17), and using Eq. (15), we find the remarkable result that the total fracton density of states on a percolating network equals

$$N_{\rm fr}(\omega)=\bar{\bar{d}}(L/a)^d(1/\omega)(\omega/\omega_{\rm FD})^{2d/(2+\theta)} . \tag{18}$$

Should we integrate Eq. (18) over the fracton frequencies, we would find,

$$\int_{\omega_{\rm co}}^{\omega_{\rm FD}}N_{\rm fr}(\omega)\,d\omega=(\bar{\bar{d}}/d)(L^d-1) , \tag{19}$$

or only $\bar{\bar{d}}/d<1$ modes per atom, and not one full mode. This reflects the missing center of mass modes of the finite clusters. The proof follows from the integration of Eq. (18) from $\omega(R)$, the smallest frequency allowed for a cluster size R, to the maximum fracton frequency ω_D,

$$\begin{aligned} \int_{\omega(R)}^{\omega_{\rm FD}}N_{\rm fr}(\omega)\,d\omega&=R^{\bar{\bar{d}}}\{1-[\omega(R)/\omega_{\rm FD}]^{\bar{\bar{d}}}\} \\ &=R^{\bar{\bar{d}}}[1-(1/R^{\bar{\bar{d}}})] \\ &=R^{\bar{\bar{d}}}-1 , \end{aligned} \tag{20}$$

which proves the statement for the normalization we have used. It is intriguing to speculate that this "missing mode" might be the analogous quantity for percolation systems that the two-level systems are for amorphous systems.

The total number of missing modes is $1-(\bar{\bar{d}}/d)$ per atom [see Eq. (19)]. Their frequencies are unknown, but their mass distribution can be calculated. There are $R^{-(1+d)}$ clusters between R and $R+dR$, leading to a mass distribution of mass $M^{-\tau}$ between $M(=R^{\bar{\bar{d}}})$ and $M+dM$, with $\tau=(d/\bar{\bar{d}})+1$. The missing mode frequencies $\Omega_{\rm tl}^M$ (tl for "two-level" systems, and M for the mass of the cluster) must be less than [from Eq. (15)]

$$\Omega_{\rm tl}^M<R_M^{-(2+\theta)/2}\propto M^{-1/\bar{\bar{d}}} . \tag{21}$$

Summarizing the results of this section, Eq. (18) exhibits the fracton density of states for a vibrational network on a percolating structure. The fracton density of states at crossover remains that of the infinite cluster:

$$N_{\rm fr}(\omega_{\rm co})=N_{\rm fr}^{\rm IC}(\omega_{\rm co})=\bar{\bar{d}}/\omega_{\rm co} , \tag{22}$$

but the slope for higher frequencies (i.e., within the fracton regime) is proportional to $\omega^{2\bar{\bar{d}}/(2+\theta)}$ instead of $\omega^{2\bar{\bar{d}}/(2+\theta)}$ for the infinite cluster alone. This is because of the contribution of finite clusters to the fracton density of states. In addition, the integral over the finite-cluster den-

sity of states shows that one mode per cluster is missing. This mode can be attributed to the center of mass motion of the cluster, and may be analogous to the "two-level systems" attributed to amorphous systems.

We also note in closing that percolating structures can easily be achieved in magnetic systems by simple dilution. A previous paper[4] showed that the diffusion equation not only maps on to the vibrational problem, but also on to the linearized spin-wave problem for ferromagnetic systems. Consequently, for randomly diluted ferromagnetic systems, the spin excitations would cross over from spin-wave-like at low energies to spin-fracton-like at higher energies, with a density of states proportional to $\omega^{\bar{d}/2+\theta-1}$ for the infinite cluster alone, and to $\omega^{d/2+\theta-1}$ for the sum of the infinite and finite clusters. Either specific heat or neutron-diffraction studies on randomly diluted ferromagnets would be interesting to compare with these forms.

IV. RELEVANCE OF FRACTON THEORY TO EXPERIMENT

We have already suggested that recent experiments on the specific heat and thermal conductivity of epoxy resins by Kelham and Rosenberg[3] may have exhibited fracton properties. They have shown (from an analysis of their specific-heat measurements) that $N(\omega)\propto\omega^2$ for $\hbar\omega/k_B<8$ K, but is proportional to ω for 8 K $<\hbar\omega/k_B<50$ K. Their figure for $N(\omega)$ appears to exhibit a discontinuity between these two regimes, though the analytic form they have chosen does not. This change of slope is exactly what one would expect if the epoxy molecules were exhibiting fractal behavior. The "crossover frequency" is chosen to be 8 K, and corresponds to a length scale of 30 Å, about the length of the epoxy molecule (diglycidyl ether of bisphenol A). For stoichiometric hardening it is also the distance between cross links of hardeners. Use of the same number of hardener molecules, but of differing lengths, did not change the crossover frequency [Nicholls and Rosenberg (unpublished)] and the crossover length scale remained the distance between cross links. This is to be expected if the epoxy molecules alone are exhibiting fractal behavior. Preliminary evidence[5] suggests that increasing the amount of hardener (i.e., reducing the distance between cross-links) tends to raise the crossover frequency. If one associates the length L in Eq. (4) with the distance between cross links, then this effect is in the correct direction. It suggests that the effect of the cross links is to restore the true Euclidean three-dimensional character of the lattice vibrations, and that the fractal behavior is to be associated with the behavior of the epoxy molecules between the connections with the hardener.

The observed power (linear) for the vibrational density of states above the hypothesized crossover frequency suggests $\bar{d}=2$. Unfortunately, at the present time we have no independent estimates for $\bar{d}$ and θ for epoxy resin. We note, however, that the length scale can be changed for the epoxy, either by changing the amount of hardener, or by using different epoxy molecules, which allows the use of Eq. (4) to determine θ. Further, $\bar{d}$ can be independently determined from x-ray scattering (see the method of Stapleton *et al.*[6]). It would be of great interest to see if $\bar{d}$ (now overdetermined) is consistent with such measurements.

There remains a problem between the analysis of the specific-heat data of Kelham and Rosenberg[3] and the theory developed above [specifically, with Eq. (11)]. Because $\bar{d}<d$, and with θ positive, $\tilde{d}<d$, so that the fracton density of states at crossover will always be less than the phonon density of states at crossover. Thus the density of states can only suffer a drop at crossover, whereas the experiments appear to exhibit a rapid rise at the frequency which we have interpreted to be crossover. We are at a loss to understand this difference in behavior. It is possible that there is an additional feature to the vibrational spectrum of epoxy resins in the fracton regime which adds a constant to the density of states, but we are unaware of its origin. As can be seen below, the analysis of the thermal conductivity is also consistent with fractal behavior above the frequency we have identified as crossover, so there is some compelling character to the evidence for fracton excitations above about 8 K in epoxy resins. However, the inconsistency with the direction of the discontinuity remains, and makes our hypothesis somewhat unsettled (see, however, the *Note added in proof*).

Perhaps a more extraordinary feature of the measurements of Kelham and Rosenberg is their finding that if one analyzes the thermal conductivity in the usual kinetic theory manner, the mean free path exhibits a precipitous drop to less than an atomic spacing above the frequency corresponding to 8 K (or the length of 30 Å). Such behavior for the effective mean free path was first noted for glasses by Zaitlin and Anderson.[7] They used a nearly vanishing mean free path [region C of their Fig. (5)] as a method for analyzing the "plateau region" found for the temperature dependences of the thermal conductivity of almost all glasses.

A mean free path of less than a lattice constant certainly suggests localized states according to the Ioffe-Regel rule.[8] We carry the fracton picture further and note that Domany *et al.* have recently shown[9] that essentially all states are localized on a Sierpinski gasket (a well-known fractal geometry[1]). In general, for fractal structures, Rammal and Toulouse[10] have recently shown that the conductance $g(L)$ scales with length for fractals as

$$g(L)\propto L^{\bar{d}-2-\theta}. \tag{23}$$

With the use of the scaling relation of Abrahams *et al.*,[11] their quantity $\beta(g)$ becomes

$$\beta(g)=\frac{d\ln g(L)}{d\ln L}=\bar{d}-2-\theta, \tag{24}$$

or, in terms of the fracton dimensionality $\bar{\bar{d}}$, using Eq. (3),

$$\beta(g)=\bar{d}[1-(2/\bar{\bar{d}})]. \tag{25}$$

The argument of Abrahams *et al.*[11] leads to localized states for $\beta\le 0$. The specific-heat analysis of Kelham and Rosenberg[3] suggests that $\bar{d}-1=1$, or $\bar{\bar{d}}=2$. Use of this

value in Eq. (25) results in $\beta(L)=0$, so that the scaling factor of Abrahams *et al.* is consistent with localized behavior.

For localized fracton states one would not expect any contribution to the thermal conductivity, but rather only a scattering of the lower-energy extended phonon states, exactly as the lower-energy two-level systems[12] have been shown to do in amorphous systems.[7] We are making a distinction here between the two-level systems which are also found in epoxy resin[3] (and in nearly all amorphous materials[7,13]) and the fracton modes. The density of states of the former are usually added to the extended phonon density of states, while the latter replace the phonons as the fundamental excitation above ω_{co} (but see our speculation concerning the origin of the "two-level systems" for percolating networks). Localized fractons would then manifest themselves by a sharp drop (vanishing) of the contribution to the thermal conductivity for excitations with $\omega > \omega_{co}$. A conventional thermal-conductivity analysis would result in a negligible mean free path in such an excitation region. The property of the epoxy resin which best maintains the correctness of our interpretation is that the frequency at which the "mean free path" becomes of the order of an atomic spacing is almost precisely the frequency at which the density of states suffers a discontinuity—crossover from a Debye-type to a fractonlike form.

At yet higher temperatures, the plateau in the thermal conductivity ends, and begins to increase (e.g., above ~ 10 K for epoxy resin). This could be caused by classical hoppinglike transitions between localized fracton states, analogous to Mott's variable range rate hopping[14] for localized electronic states. We have not as yet carried through a detailed analysis for thermal transport in such a regime.

The fracton hypothesis suggests that materials exhibiting a significant temperature spread for the plateau regime, in the thermal conductivity, possess a characteristic length considerably larger than an atomic spacing between which vibrational excitations are localized (we hypothesize, fractonlike). For longer-length scales, one passes into the normal Debye-type regime. The width of the plateau region will increase as the crossover length L increases.

It is interesting to compare the results and analysis of Kelham and Rosenberg[3] on epoxy resin with that of Zaitlin and Anderson[7] on other noncrystalline materials (a borosilicate glass and a polycarbonate). As recognized by Kelham and Rosenberg, Zaitlin and Anderson were the first to associate the plateau in the thermal conductivity of almost all glasses (see Zeller and Pohl[13]) with a sudden drop in the phonon mean free path for frequencies above a minimum ω_0 (the crossover frequency?). This is clearly exhibited in their Fig. 5, region C. The similarity of their analysis for noncrystalline materials, and that of Kelham and Rosenberg for epoxy resin, where long-range correlations (~ 30 Å) are expected, is striking.

We admit that it is a little puzzling why ordinary glasses should exhibit such a length, roughly independent of the character of their constituents. However, our analysis would not be the first to argue for such extended correlations. For example, Morgan and Smith[15] have made similar arguments (even to lengths up to 1000 Å), though with a very different model in mind.

It is interesting to note that as pointed out by Morgan and Smith the plateau temperature width is much larger for amorphous Se than for most glasses (Zeller and Pohl[13]). It is known that the characteristic correlation length in amorphous Se is much longer than in most glasses. We have already noted this phenomenon above for epoxy resin. Finally, Phillips[16] has also argued for extended correlations in amorphous systems.

Recent irradiation experiments on crystalline quartz also tend to confirm our interpretation of fractal behavior in glasses. Laermans *et al.*[17] have shown that electron irradiation of crystalline quartz does not produce a plateau region in the thermal conductivity. However, neutron irradiation does generate a plateau regime with a width slightly larger for larger neutron doses.[18] X-ray scattering by Grasse *et al.*[19] shows that neutron irradiation causes amorphous regions of diameter 20 Å, while Grasse *et al.*[20] show that electron damage does not, hence the lack of a plateau region in the thermal conductivity for the latter. Finally, Grasse *et al.*[21] point out that the size of the amorphous regime tends to grow slightly (20%) with increasing neutron irradiation. This is consistent with the slight increase in plateau length found by de Goer *et al.*[18] as a function of increasing neutron dosage.

V. SUMMARY AND CONCLUSIONS

In summary, we contend that the thermal properties of epoxy resin and glasses can be understood on the basis of a crossover from Debye-type behavior at low frequencies to fracton behavior at higher frequencies. The density of states correspondingly changes the exponent of its power law from $d-1$ to $\bar{d}-1$ [Eq. (2)]. At this same crossover frequency, the vibrational states change their character from extended to localized, thereby profoundly affecting the thermal transport and serving as a possible explanation for the extremely small mean free path of phonons in this energy region as extracted from more conventional analyses. The crossover frequency is proportional to the inverse of the length scale, according to Eq. (4), fracton behavior expected for shorter lengths. Any increase in this length should therefore reduce the crossover energy and increase the width of the plateau region measured in thermal-conductivity experiments.

Note added in proof. The form we have used for the normalized fracton density of states assumed that the force constant and mass scaled smoothly through the crossover regime. Recent work of P. F. Tua, S. J. Putterman, and R. Orbach [Phys. Lett. (in press)] suggests an alternative picture: a drop in ω vs inverse length scale at the crossover length. This leads to a jump in the density of states (instead of a drop), going from the phonon to fracton regimes. Excellent agreement with the experimental results of Ref. 3 is obtained. Finally, an effective medium approximation for $N(\omega)$ has been obtained very recently for percolating networks by B. Derrida, R. Orbach, and Kin-Wah Yu (unpublished). It strongly supports the assumptions of Tua *et al.*, giving additional con-

fidence to a fracton interpretation for short-length scale vibrational excitations in amorphous materials.

ACKNOWLEDGMENTS

The authors wish to acknowledge a remarkable initial conversation with Professor A. Schmid, who asked whether fractal behavior might not have relevance to epoxy-resin properties, and valuable assistance from Professor G. Toulouse for his application of localization scaling to the fractal problem. We also wish to thank Professor T. C. Lubensky and Dr. R. Rammal for very helpful conversations. The research of one of us (R.O.) was supported in part by the U.S. Navy Office of Naval Research Contract No. Nonr N00014-75-C-0245, and that of two of us (S.A. and R.O.) in part by the U.S. National Science Foundation Grant No. DMR 81-15542.

---

*Permanent address: The Racah Institute, The Hebrew University, Jerusalem 9100, Israel.

†Permanent address: Laboratorium voor Vaste Stof- en Hoge Druk-Fysika, Katholieke Universiteit Leuven, Celestijnenlaan 200D, B-3030 Leuven, Belgium.

‡Permanent address: Physics Department, University of California, Los Angeles, CA 90024.

§Permanent address: Clarendon Laboratory, University of Oxford, Parks Road, Oxford OX1 3PU, England.

[1]B. B. Mandelbrot, *The Fractal Geometry of Nature* (Freeman, San Francisco, 1982); see also Sci. Am. 238 (4), 16 (1978); Ann. Isr. Phys. Soc. 5, 59 (1983).

[2]S. Alexander and R. Orbach, J. Phys. (Paris) Lett. 43, L-625 (1982).

[3]S. Kelham and H. M. Rosenberg, J. Phys. C 14, 1737 (1981).

[4]S. Alexander, J. Bernasconi, W. R. Schnieder, and R. Orbach, Rev. Mod. Phys. 53, 175 (1981).

[5]D. E. Farrell, J. E. de Oliveira, and H. M. Rosenberg (unpublished).

[6]H. J. Stapleton, J. P. Allen, C. P. Flynn, D. G. Stinson, and S. R. Kurtz, Phys. Rev. Lett. 45, 1456 (1980); J. P. Allen, J. T. Colvin, D. G. Stinson, C. P. Flynn, and H. J. Stapleton, Biophys. J. 38, 299 (1982).

[7]M. P. Zaitlin and A. C. Anderson, Phys. Rev. B 12, 4475 (1975).

[8]A. F. Ioffe and A. R. Regel, Prog. Semicond. 4, 237 (1960).

[9]E. Domany, S. Alexander, D. Bensimon, and L. P. Kadanoff, Phys. Rev. B 28, 3110 (1983).

[10]R. Rammal and G. Toulouse, J. Phys. (Paris) Lett. 44, L-13 (1983).

[11]E. Abrahams, P. W. Anderson, D. C. Licciardello, and T. V. Ramakrishnan, Phys. Rev. Lett. 42, 673 (1979).

[12]W. A. Philips, J. Low Temp. Phys. 7, 351 (1972); P. W. Anderson, B. I. Halperin, and C. M. Varma, Philos. Mag. 25, 1 (1972).

[13]R. C. Zeller and R. O. Pohl, Phys. Rev. B 4, 2029 (1971).

[14]N. F. Mott, Philos. Mag. 19, 835 (1969).

[15]G. J. Morgan and D. Smith, J. Phys. C 7, 649 (1974).

[16]J. C. Phillips, J. Non-Cryst. Solids 34, 153 (1979); 43, 37 (1981); Phys. Today 35 (2), 27 (1982), Bull. Am. Phys. Soc. 28, 398 (1983).

[17]C. Laermans, A. M. de Goer, and M. Locatelli, Phys. Lett. 80A, 331 (1980).

[18]R. Berman, Proc. R. Soc. London Ser. A 208, 90 (1951); and A. M. de Goer, M. Locatelli, and C. Laermans, J. Phys. (Paris) Colloq. 42, C6-78 (1981). For similar effects in synthetic sapphires, see R. Berman, E. L. Foster, and H. M. Rosenberg, *Defects in Crystalline Solids—Report of the 1954 Bristol Conference* (Physical Society, London, 1954), p. 321.

[19]D. Grasse, O. Kocar, H. Peisl, S. C. Moss, and B. Golding, Phys. Rev. Lett. 46, 261 (1981).

[20]D. Grasse, D. Muller, H. Peisl, and C. Laermans, J. Phys. (Paris), Colloq. 43, C9-119 (1982).

[21]D. Grasse, O. Kocar, H. Peisl, and S. C. Moss, Radiat. Eff. 66, 61 (1982).

PHYSICAL REVIEW B VOLUME 27, NUMBER 8 15 APRIL 1983

Frequency dependence of the conductivity in presence of an electric field in one dimension: Weak-disorder limit

B. Derrida
Service de Physique Théorique, Centre d'Etudes Nucléaires de Saclay, 91191 Gif-sur-Yvette Cedex, France

R. Orbach*
Ecole Supérieure de Physique et de Chimie industrielles de Paris 10 rue Vauquelin, 75005 Paris, France
(Received 20 September 1982)

The frequency dependence of the electrical conductivity is examined for a classical hopping model of a random one-dimensional system in the presence of a superposed static electric field. The effect of the field is taken as a constant bias for the left-right jump rates. A general expression is derived for the mean velocity and frequency-dependent conductivity. Explicit evaluation of these equations is given for correlated and uncorrelated hopping rates: (1) in general for high frequencies and (2) to lowest order in the disorder for all frequencies. In the latter case, an initial decrease in $\sigma(\omega)$ for very small ω is found, $\sigma_R = a_0 - a_1\omega^2$, $\sigma_I = a_2\omega^3$. For larger frequencies, the conductivity crosses over to the form $\sigma(\omega) = b_0 + b_1(i\omega)^{1/2}$, previously calculated by Alexander and Orbach. The a_i, b_i are constants which depend on the strength of the bias and the randomness. The crossover frequency increases with the bias. In addition, the variance in the autocorrelation function is calculated in the long-time limit, for weak disorder in the symmetric case. It is shown that fluctuations do not significantly affect the determination of this quantity under these conditions.

I. INTRODUCTION

The frequency dependence of the electrical conductivity in one-dimensional systems with symmetrical random hopping rates has been calculated recently in a series of papers.[1-3] Recent electrical conductivity experiments on the quasi-one-dimensional conductor quinolinium ditetracyanoquinodimethanide [Qn(TCNQ)$_2$] have been analyzed using these results by Alexander *et al.*[4] All of these studies, with the exception of Ref. 3, have only treated the case of symmetric hopping rates, and hence were only applicable in the small electric field regime.

Recently, attention has been directed to the question of transport with random, but biased, hopping rates.[5-7] These calculations have explored the time dependence of the mean displacement. Our purpose is to calculate the frequency dependence of the conductivity in the nonlinear electric field regime. We shall find a result very different from the symmetric case at the lowest of frequencies, crossing over to a response which is the same as found for symmetric hopping at higher frequencies. This crossover has been anticipated in Ref. 3.

Our purpose here is to formulate the problem in such a manner that the frequency dependence of the conductivity can be calculated directly. Section II describes the formal calculation of the ac conductivity in a uniform dc field. Section III exhibits the high-frequency limit for the conductivity. The solution for weak disorder is developed in Sec. IV, with figures exhibiting the real and imaginary part of the frequency response for different biases. In both Secs. III and IV we treat the case of correlated and uncorrelated hopping rates. In Sec. V, we derive an expression for the variance of the autocorrelation function in the weak-disorder limit, and show that fluctuations are unimportant in this, and the long-time, limit. Finally, we summarize our findings in Sec. VI.

II. FORMAL SOLUTION FOR THE ac CONDUCTIVITY IN A UNIFORM dc FIELD

We treat the same master equation for hopping transfer as in Ref. 1, but with asymmetric hopping rates. Let $P_n(t)$ be the probability that site n is occupied at time t. Then, for near-neighbor hops only,

$$\frac{dP_n}{dt} = Y_{n+1}P_{n+1} + X_{n-1}P_{n-1} - (X_n + Y_n)P_n \ , \tag{1}$$

where Y_{n+1} is the hopping rate to the left (from $n+1$ to n) and X_{n-1} is the hopping rate to the right (from $n-1$ to n). In the presence of an applied static electric field $\mathscr{E}_0$, and a small oscillating field $\mathscr{E}$ at frequency ω,

$$Y_n = \left[\exp\left[-\frac{(\mathscr{E}_0 + \mathscr{E}e^{i\omega t})el}{k_B T}\right]\right] W_n$$
$$\equiv \left[\exp\left[-2\frac{(\mathscr{E}_0 + \mathscr{E}e^{i\omega t})el}{k_B T}\right]\right] X_{n-1} \ , \tag{2}$$

where we have taken the potential drop to be the same along all segments of equal length l, and where W_n is the symmetric hop rate between $n-1$ and n (i.e., the hop rate in the absence of an applied static field). Expanding in $\mathscr{E}$,

$$Y_n = a(1 - Ee^{i\omega t})X_{n-1} \ , \tag{3}$$

where $E = 2\mathscr{E}el/k_B T$ and $a = \exp(-2\mathscr{E}_0 el/k_B T)$ is termed the bias. The velocity of the particle at time t is given by

$$V = \frac{d}{dt}\frac{\sum_n nP_n(t)}{\sum_n P_n(t)}$$
$$= \frac{\sum_n (X_n - Y_n)P_n(t)}{\sum_n P_n(t)} \ . \tag{4}$$

Expanding $P_n(t)$ in a power series in the reduced field E,

$$P_n(t) = Q_n + R_n Ee^{i\omega t} + \cdots \ , \tag{5}$$

one can derive expressions for Q_n and R_n from Eq. (1). One finds

$$X_n(aQ_{n+1} - Q_n) - X_{n-1}(aQ_n - Q_{n-1}) = 0 \ , \tag{6a}$$

$$i\omega R_n = X_n(aR_{n+1} - R_n) - X_{n-1}(aR_n - R_{n-1})$$
$$- aX_n Q_{n+1} + aX_{n-1}Q_n \ . \tag{6b}$$

Once Q_n and R_n are known, we may find V from Eqs. (5) and (4). From Eq. (6b), $\sum_n R_n = 0$ whence

$$V = \frac{\sum_n \{[X_n - aX_{n-1}(1 - Ee^{i\omega t})][Q_n + R_n Ee^{i\omega t}]\}}{\sum_n Q_n} \ . \tag{7}$$

Writing the velocity in the form $V = v + Ee^{i\omega t}\sigma(\omega)$, one identifies

$$v = \frac{\sum_n [(X_n - aX_{n-1})Q_n]}{\sum_n Q_n} \tag{8}$$

and

$$\sigma(\omega) = \frac{\sum_n [(X_n - aX_{n-1})R_n + aX_{n-1}Q_n]}{\sum_n Q_n} \ . \tag{9}$$

These are our two principal relationships (the first is merely a restatement of the result obtained in Refs. 5–7). We can evaluate Eq. (8) immediately for our model. Expressing the Q_n as

$$Q_n = \sum_{p=0}^{\infty} a^p / X_{n+p} \ , \tag{10}$$

Equation (6a) is solved immediately. One finds

$$v = (1-a)\Big/\left\langle \frac{1}{X_0} \right\rangle \ . \tag{11}$$

This is the same result as in Ref. 7, if we note $a = \exp(-2\mathscr{E}_0 el/k_B T)$ and $\langle 1/X_0 \rangle = \exp(\mathscr{E}_0 el/k_B T)\langle 1/W \rangle$, where W_n is the symmetric hop rate between $n-1$ and n in the absence of an applied electric field. Inserting into Eq. (11),

$$v = 2\langle 1/W \rangle^{-1} \sinh(\mathscr{E}_0 el/k_B T) \ , \tag{12}$$

a well-known result,[7] and one which reproduces Rice *et al.*[8] for the case of a regular lattice. We now go on to explicit evaluation of the conductivity, Eq. (9), in the high-frequency (Sec. III) and weak-disorder (Sec. IV) regimes.

III. HIGH-FREQUENCY LIMIT

We examine the case when the frequency ω is much greater than any of the hopping rates X_n, Y_n. Using the relationship Eq. (6b), one expands in inverse powers of ω to find R_n in terms of Q_n:

$$R_n = \frac{1}{i\omega}a(X_{n-1}Q_n - X_n Q_{n+1}) + \frac{1}{(i\omega)^2}(a^2 X_n^2 Q_{n+1} - a^2 X_n X_{n+1}Q_{n+2} - aX_n X_{n-1}Q_n + aX_n^2 Q_{n+1} - a^2 X_{n-1}^2 Q_n$$
$$+ a^2 X_{n-1}X_n Q_{n+1} + aX_{n-1}X_{n-2}Q_{n-1} - aX_{n-1}^2 Q_n) + O\left[\frac{1}{(i\omega)^3}\right] \ . \tag{13}$$

One now uses the expression for Q_n, Eq. (10), in Eq. (13) to obtain the explicit form for R_n. Knowing Q_n and R_n, $\sigma(\omega)$ is known from Eq. (9). We exhibit two forms for $\sigma(\omega)$: the X_n uncorrelated, and the X_n correlated. The former becomes

$$\sigma_{\text{uncor}}(\omega)=a\langle X\rangle+\frac{1}{i\omega}[2a^2\langle X\rangle^2-a(a+1)\langle X^2\rangle+a(1-a)\langle X\rangle/\langle 1/X\rangle]$$
$$+\frac{1}{(i\omega)^2}[2a^3\langle X\rangle^3-3a^2(1+a)\langle X\rangle\langle X^2\rangle+a(1+a)^2\langle X^3\rangle-a(1-a)\langle X^2\rangle/\langle 1/X\rangle]+\cdots . \tag{14}$$

This expansion is, in principle, valid as long as $\omega\gg\langle X^n\rangle^{1/n}$. This is an interesting form, in that some unusual averages enter for asymmetric transfer rates ($a<1$). For the symmetric case, $a=1$, and one recovers the high-frequency form for $\sigma(\omega)$ given in Ref. 1 [their Eq. (7.8)]. It is interesting to note that the inverse moment of the X_n enters at high frequencies in the asymmetric case. This suggests nonuniversal behavior for distribution of class (c) (in the notation of Ref. 1) even at high frequencies, whereas the behavior is purely universal in the high-frequency regime for symmetric transfer rates.

The correlated case has the following high-frequency conductivity:

$$\sigma_{\text{cor}}(\omega)=[(1-a)/\langle 1/X\rangle]\sum_{p=1}^{\infty}\langle X_0/X_p\rangle a^p$$
$$+\frac{1}{i\omega}[(1-a)/\langle 1/X\rangle]\left[a\langle X\rangle+2\sum_{p=2}^{\infty}\langle X_0X_1/X_p\rangle a^p-(1+a)\sum_{p=1}^{\infty}\langle X_0^2/X_p\rangle a^p\right]+\cdots , \tag{15}$$

if $\omega\gg\langle X^n\rangle^{1/n}$. Because of the translational invariance, one can replace averages like $\langle X_0X_1/X_p\rangle$ by $\langle X_nX_{n+1}/X_{n+p}\rangle$ for any n.

In the symmetric limit ($a=1$) for short-range (sr) correlations, it reduces to

$$\sigma_{\text{cor, sr}}(\omega)=\langle X\rangle+\frac{2}{i\omega}[\langle X_0X_1\rangle-\langle X_0^2\rangle]+\cdots , \quad \omega\gg\langle X^n\rangle^{1/n} . \tag{16}$$

IV. WEAK-DISORDER LIMIT

We pass to the limit of weak disorder in order to obtain a solution of Eq. (6b). To this order the expression for the frequency-dependent conductivity developed below [e.g., Eq. (23)] is exact for all frequencies (see the Summary, Sec. VI, for further discussion of this question). We set

$$\frac{1}{X_n}=A+\epsilon_n, \quad \langle\epsilon_n^2\rangle^{1/2}\ll A . \tag{17}$$

In exactly the same manner as before, we can write the exact solution for Q_n,

$$Q_n=A/(1-a)+\sum_{p=0}^{\infty}a^p\epsilon_{n+p} . \tag{10'}$$

We must now evaluate R_n in terms of the Q_n from Eq. (6b). To carry this through (to any order in ϵ, $\sum_{n=-\infty}^{n=\infty}R_n=0$), we expand,

$$R_n=\sum_{p=-\infty}^{\infty}\beta_p\epsilon_{n+p}$$
$$+\sum_{p=-\infty}^{\infty}\sum_{q=-\infty}^{\infty}\gamma_{p,q}\epsilon_{n+p}\epsilon_{n+q}+\cdots , \tag{18}$$

where we shall work only to linear order in ϵ. Using Eqs. (10') and (18) in Eq. (9), one finds to lowest order in the disorder, for uncorrelated X_n,

$$\sigma_{\text{uncor}}(\omega)=[(1-a)/A]$$
$$\times\{(1/A^2)(a\beta_{-1}-\beta_0)\langle\epsilon^2\rangle$$
$$+a/(1-a)$$
$$+[a/(1-a)A^2]\langle\epsilon^2\rangle\} , \tag{19}$$

where it remains necessary to calculate the β_p defined in Eq. (18). The algebra leading to a solution is tedious, and we merely exhibit the results here. For $p\geq 0$,

$$\beta_p=\frac{\lambda(a-1)}{(\lambda-1)(\lambda-a)}a^p$$
$$+\frac{(\lambda-a)^2}{(1-a)(\lambda-1)(\lambda^2-a)}\mu^p , \tag{20a}$$

and for $p\leq -1$,

$$\beta_p=-\frac{a(\lambda-1)^2}{(\lambda-a)(1-a)(\lambda^2-a)}\lambda^{p+1} , \tag{20b}$$

where λ is the largest root of

$$\lambda^2-\lambda(1+a+i\omega A)+a=0\ , \tag{21}$$

$\mu=a/\lambda$, and $a\leq 1$. In particular, for purposes of Eq. (19),

$$a\beta_{-1}-\beta_0=\frac{a}{1-a}\frac{a+1-2\lambda}{\lambda^2-a}\ , \tag{22}$$

leading to our principal result,

$$\sigma_{\text{uncor}}(\omega)=\frac{a}{A}+\frac{\langle\epsilon^2\rangle}{A^3}\frac{a(\lambda-1)^2}{\lambda^2-a}\ . \tag{23}$$

The frequency limits of Eq. (23) are interesting, and illuminate the essential physics of the transport process. The behavior of the roots of Eq. (21) are essential to our analysis. If one attempts to make a low-frequency expansion of λ, one is faced with a comparison of $(1-a)^2$ to $\omega A(1+a)$.

$$2\lambda=1+a+i\omega A$$
$$+[(1-a)^2+2i\omega A(1+a)-(\omega A)^2]^{1/2}\ . \tag{24}$$

Our analysis of this ratio is based on a comparison of the "drift" distance with the "diffusive" displacement, exactly as in Ref. 3. We shall show that the very small ω (long-time) limit is dominated by the drift of the particle under the influence of the electric field, the larger ω domain by diffusion. The former will result in a diminution of $\sigma_{\text{uncor}}(\omega)$ with increasing frequency, the latter in an increase. The former is a consequence of electric field driven drift causing the particle to encounter rare very small transfer rates which diminish the conductivity. It would not have experienced these transfers if its motion were purely diffusive on the same time scale of $1/\omega$. The latter regime is associated with shorter and shorter root-mean-square distances as ω increases, leading to fewer encounters with small transfer rates.

The crossover condition can be obtained in exactly the same manner as in Ref. 3 by calculation of the relevant lengths. The drift velocity has already been derived in Eq. (11). Approximating (weak disorder) $\langle 1/X\rangle=A$, in a time $1/\omega$, the particle experiences a net average displacement

$$l_{\text{drift}}=(1-a)/\omega A\ . \tag{25a}$$

Likewise, on the same time scale, the particle's root-mean-square diffusive distance is

$$l_{\text{diff}}=(A\omega)^{-1/2}\ . \tag{25b}$$

The ratio of the square of the two is

$$l^2_{\text{drift}}/l^2_{\text{diff}}=[(1-a)^2/A^2\omega^2]/[1/A\omega]\ ,$$

or, more simply $(1-a)^2/A\omega$ which, for small $1-a$, is precisely the ratio Eq. (24). Hence, the crossover in frequency behavior can be traced to the same origin as for nonlinear electric field effects as discussed in Ref. 3.

For the first regime (lowest ω), one finds

$$\sigma_{\text{uncor}}(\omega)\sim a_0-a_1\omega^2+a_2 i\omega^3+\cdots\ , \qquad \omega<(1-a)^2/A\ , \tag{26}$$

while for the latter regime,

$$\sigma_{\text{uncor}}(\omega)\sim b_0+b_1(i\omega)^{1/2}+\cdots\ , \qquad \omega>(1-a)^2/A\ . \tag{27}$$

The coefficients are positive, and depend on the strength of the disorder through Eq. (23). The limiting behaviors are easily seen if one plots the full solution to Eq. (23). Taking $A=1$ for simplicity, we have calculated the frequency-dependent part of $\sigma(\omega)$, $(\lambda-1)^2/(\lambda^2-a)$, against ω, for $a=0.8$ and 0.9. Figure 1 exhibits the real part of this factor for the interesting frequency regime with $a=0.8$. One sees a crossover at $\omega=0.046$ between the two-frequency regimes. The low-frequency drift-dominated limiting regime for the frequency-dependent part of $\sigma(\omega)$ is exhibited in Fig. 2, and for the imaginary part in Fig. 3. Finally, the higher-frequency diffusion-dominated regime-limiting behavior is exhibited in Fig. 4. Similar plots for $a=0.9$ are exhibited in Figs. 5–7. One sees that crossover takes place at lower frequency, $\omega=0.011$ from Fig. 5. This follows closely the prediction of Eq. (24) (as it must).

These curves show that the limiting low-frequency dependence is an immediate and strong function of the nonlinear response. For small elec-

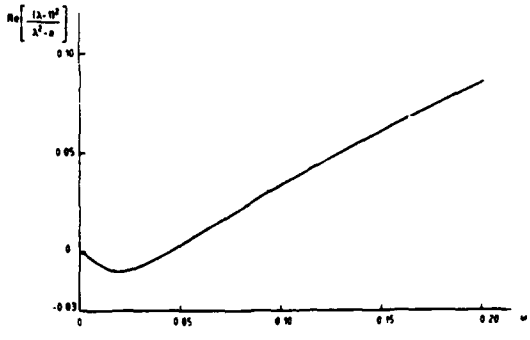

FIG. 1. Plot of the real part of the frequency-dependent part of $\sigma(\omega)$, $(\lambda-1)^2/(\lambda^2-a)$ (defined in the text), vs ω for the bias parameter $a=0.8$, and background regular inverse hop rate $A=1$. Note the crossover behavior near $\omega=0.046$.

tric fields, the drift regime is limited to very small frequencies, increasing in scale as the electric field is enhanced. For the symmetric case, $a=1$, we recover precisely the expression for $\sigma_{\text{uncor}}(\omega)$ given in Refs. 2 and 9, to lowest order in ω.

For correlated X_n, the argument goes through as before, with the following results for the symmetric case ($a=1$):

$$\sigma_{\text{cor}}(\omega)=1/A+\frac{\langle\epsilon_0^2\rangle}{A^3}\left[\frac{\lambda-1}{\lambda+1}\right] +2\frac{\lambda-1}{\lambda+1}\frac{1}{A^3}\sum_{p=1}^{\infty}\langle\epsilon_0\epsilon_p\rangle\frac{1}{\lambda^p}\,, \tag{28}$$

and the asymmetric case ($a<1$):

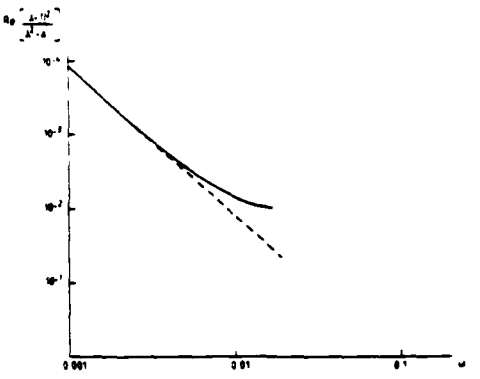

FIG. 2. Same as for Fig. 1, but for small ω on an expanded scale. The straight dashed line has slope 2, showing that $\sigma_R(\omega)$ falls off as ω^2 for smallest ω.

$$\sigma_{\text{cor}}(\omega)=\frac{a}{A}+\frac{\langle\epsilon_0^2\rangle}{A^3}\frac{a(\lambda-1)^2}{\lambda^2-a}+\frac{1}{A^3}\sum_{p=1}^{\infty}\langle\epsilon_0\epsilon_p\rangle\left[\frac{(\lambda-a)^2}{\lambda^2-a}\frac{a^p}{\lambda^p}+\frac{a(\lambda-1)^2}{\lambda^2-a}\frac{1}{\lambda^p}-(1-a)a^p\right]. \tag{29}$$

V. FLUCTUATIONS IN THE AUTOCORRELATION FUNCTION

One of the more intriguing questions which exact treatments of random one-dimensional systems have been unable to treat is fluctuations about the ensemble average. The simplest quantity, the autocorrelation function, is an example of how difficult such problems are. As discussed in Ref. 1, Sec. X, the variance of the autocorrelation function $P_0(t)$, involves the calculation of

$$\langle P_0^2(t)\rangle=\mathcal{L}^{-1}\left\langle\frac{1}{2\pi i}\int_{c-i\infty}^{c+i\infty}d\omega'\tilde{P}_0(\omega')\tilde{P}_0(\omega-\omega')\right\rangle, \tag{30}$$

where $\tilde{P}_0(\omega)$ is the Laplace transform ($\mathcal{L}$) of $P_0(t)$, where

$$\tilde{P}_n(\omega)=\int_0^{\infty}e^{-\omega t}P_n(t)dt\,.$$

Because the $\tilde{P}_n(\omega)$ are correlated[1] for different ω, the averaging process in Eq. (30) does not commute with the convolution, and one cannot simplify fur-

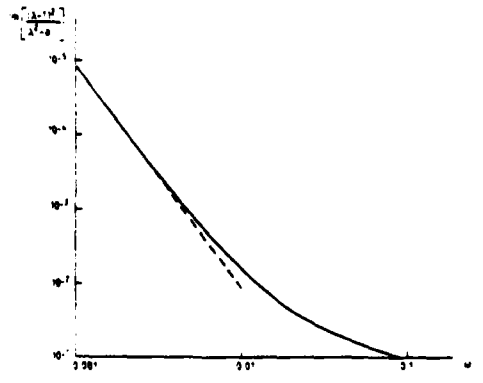

FIG. 3. Same as for Fig. 1, but for the imaginary part of $\sigma(\omega)$, $\sigma_I(\omega)$, for small ω on an expanded scale. The straight dashed line has slope 3, showing that $\sigma_I(\omega)$ increases as ω^3 for the smallest ω.

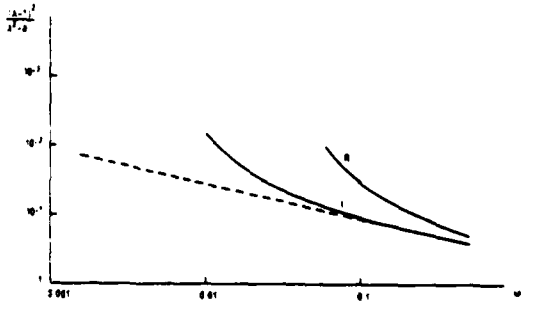

FIG. 4. Same as for Fig. 1, but for the real (R) and imaginary (I) parts of $(\lambda-1)^2/(\lambda^2-a)$ above the crossover frequency on an expanded scale. The straight line has slope $\frac{1}{2}$, showing that $\sigma_I(\omega)$ rapidly reaches this limiting behavior, but $\sigma_R(\omega)$ does so more slowly.

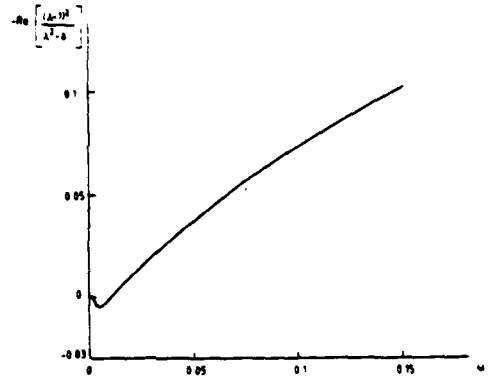

FIG. 5. Plot of the real part of the frequency-dependent part of $\sigma(\omega)$, $(\lambda-1)^2/(\lambda^2-a)$ (defined in the text), vs ω for the bias parameter $a=0.9$, and background regular inverse hop rate $A=1$. Note the crossover behavior near $\omega=0.011$.

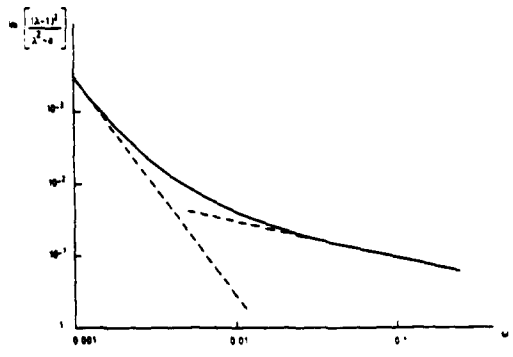

FIG. 6. Same as for Fig. 5, but for $\sigma_I(\omega)$ on an expanded scale. The straight dashed lines have slopes 3 and $\frac{1}{2}$, for comparison with limiting behaviors of $\sigma_I(\omega)$ for frequencies below and above crossover, respectively.

ther that expression.

Using the approximation of weak disorder, we have been able to make some progress. The Laplace transform of Eq. (1), with the initial condition that the particle is at the origin, $n=0$ at time $t=0$, is

$$\omega\tilde{P}_n(\omega)=\delta_{n,0}+X_n[a\tilde{P}_{n+1}(\omega)-\tilde{P}_n(\omega)] + X_{n-1}[\tilde{P}_{n-1}(\omega)-a\tilde{P}_n(\omega)] . \quad (31)$$

As before, we expand in the ϵ_n:

$$\tilde{P}_n(\omega)=\tilde{Q}_n(\omega)+\sum_{p=-\infty}^{\infty}\alpha_{n,p}\epsilon_p + \sum_{p=-\infty}^{\infty}\sum_{q=-\infty}^{\infty}\beta_{n,p,q}\epsilon_p\epsilon_q+\cdots , \quad (32)$$

where $\tilde{Q}_n$, $\alpha_{n,p}$, and $\beta_{n,p,q}$ are all functions of ω. A little algebra shows that if the X_n are not correlated,

$$\langle\tilde{P}_n(\omega)\tilde{P}_n(\omega')\rangle-\langle\tilde{P}_n(\omega)\rangle\langle\tilde{P}_n(\omega')\rangle=\langle\epsilon^2\rangle\sum_{p=-\infty}^{\infty}\alpha_{n,p}(\omega)\alpha_{n,p}(\omega') , \quad (33)$$

the $\beta_{n,p,q}$ cancel when taking the difference (33). We need only find the $\alpha_{n,p}(\omega)$ to solve Eq. (33). These are found as before by use of Eq. (32) in Eq. (31). One finds the relations

$$\omega\tilde{Q}_n=\delta_{n,0}+(1/A)(a\tilde{Q}_{n+1}-\tilde{Q}_n+\tilde{Q}_{n-1}-a\tilde{Q}_n) \quad (34a)$$

and

$$\omega\alpha_{n,p}=(1/A)[a\alpha_{n+1,p}+\alpha_{n-1,p}-(1+a)\alpha_{n,p}] -(1/A^2)\delta_{n,p}(a\tilde{Q}_{n+1}-\tilde{Q}_n)-(1/A^2)\delta_{n-1,p}(\tilde{Q}_{n-1}-a\tilde{Q}_n) . \quad (34b)$$

If λ and μ are the two roots of

$$a\lambda^2-\lambda(1+a+A\omega)+1=0 , \quad (35)$$

with $|\lambda|>|\mu|$, then the $\tilde{Q}_n$ are given by

$$n\geq 0:\ \tilde{Q}_n=A\lambda\mu^{n+1}/(\lambda-\mu),\quad n\leq 0:\ \tilde{Q}_n=A\lambda^{n+1}\mu/(\lambda-\mu) .$$

The $\alpha_{n,p}$ are likewise given by

$$p \geq 0, \quad \alpha_{n,p} = \begin{cases} -\dfrac{\lambda\mu}{(\lambda-\mu)^2}(\lambda-1)(1-\mu)\mu^n, & n \geq p+1 \\ \dfrac{\mu^2(\lambda-1)^2}{(\lambda-\mu)^2}\mu^p\lambda^{n-p}, & n \leq p \end{cases}$$

and for

$$p \leq -1, \quad \alpha_{n,p} = \begin{cases} \dfrac{(1-\mu)^2\lambda^2}{(\lambda-\mu)^2}\lambda^p\mu^{n-p}, & n \geq p+1, \\ -\dfrac{\lambda\mu}{(\lambda-\mu)^2}(\lambda-1)(1-\mu)\lambda^n, & n \leq p . \end{cases}$$

Using these expressions, Eq. (33) becomes

$$\langle \tilde{P}_0(\omega)\tilde{P}_0(\omega')\rangle - \langle \tilde{P}_0(\omega)\rangle\langle \tilde{P}_0(\omega')\rangle = \langle \epsilon^2 \rangle \frac{\lambda_1\lambda_2\mu_1\mu_2[(\lambda_1-1)^2(\lambda_2-1)^2\mu_1\mu_2+\lambda_1\lambda_2(1-\mu_1)^2(1-\mu_2)^2]}{(\lambda_1-\mu_1)^2(\lambda_2-\mu_2)^2(\lambda_1\lambda_2-\mu_1\mu_2)}, \tag{36}$$

where λ_1,μ_1 and λ_2,μ_2 are the roots of Eq. (35) (remembering $|\lambda| > |\mu|$) for ω and ω', respectively. For the symmetric case, $a=1$ and Eq. (36) "simplifies" to ($\mu_1=1/\lambda_1$, $\mu_2=1/\lambda_2$),

$$\langle \tilde{P}_0(\omega)\tilde{P}_0(\omega')\rangle - \langle \tilde{P}_0(\omega)\rangle\langle \tilde{P}_0(\omega')\rangle = \langle \epsilon^2 \rangle \frac{2\lambda_1^2\lambda_2^2}{(\lambda_1+1)^2(\lambda_2+1)^2(\lambda_1^2\lambda_2^2-1)} . \tag{37}$$

We wish the inverse Laplace transform of this expression, a formidable task which so far has eluded us for general ω,ω'. However, for small ω,ω', $\lambda = 1 + (A\omega)^{1/2}$, whence Eq. (37) reduces to

$$\langle \tilde{P}_0(\omega)\tilde{P}_0(\omega')\rangle - \langle \tilde{P}_0(\omega)\rangle\langle \tilde{P}_0(\omega')\rangle = \frac{\langle \epsilon^2 \rangle}{16\sqrt{A}\,(\sqrt{\omega}+\sqrt{\omega'})} . \tag{38}$$

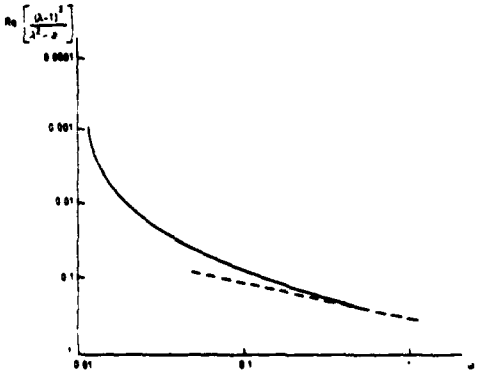

FIG. 7. Same as for Fig. 5, but for the real part of $(\lambda-1)^2/(\lambda^2-a)$ above the crossover frequency on an expanded scale. The straight dashed line has slope $\frac{1}{2}$ for comparison with the predicted limiting behavior.

The inverse Laplace transform of $(\sqrt{\omega}+\sqrt{\omega'})^{-1}$ is known, so that the long-time behavior of the variance of $P_0(t)$ is approximately given by

$$\langle P_0^2(t)\rangle - \langle P_0(t)\rangle^2 = \frac{\langle \epsilon^2 \rangle}{64\sqrt{2\pi}\sqrt{A}} t^{-3/2}, \quad t \to \infty . \tag{39}$$

Comparing with $\langle P_0(t)\rangle = \sqrt{A}/(2\sqrt{\pi}t^{1/2})$, we find

$$\frac{\langle P_0^2(t)\rangle - \langle P_0(t)\rangle^2}{\langle P_0(t)\rangle^2} = \frac{\sqrt{\pi}}{16\sqrt{2}} \frac{\langle \epsilon^2 \rangle}{A^2} \left[\frac{A}{t}\right]^{1/2}, \quad t \to \infty . \tag{40}$$

This is a highly satisfying result, for it demonstrates that the relative variance of $P_0(t)$ falls off with increasing time as $t^{-1/2}$ for the symmetric case with weak disorder. The asymmetric case is more complicated, but it is at least formulated [Eq. (36)] in terms of the Laplace transformed quantities. The full problem, for arbitrary disorder, seems out of reach at present.

VI. SUMMARY

We have considered the random one-dimensional near-neighbor hopping transport problem for asymmetric hopping rates with constant bias. This would correspond to the problem of measurement of the frequency-dependent conductivity in the presence of

a large dc electric field. We have derived expressions for the drift velocity and $\sigma(\omega)$ and have evaluated them

(a) exactly for the drift velocity contribution to the dc conductivity,
(b) exactly in the high-frequency limit, and
(c) exactly for weak disorder.

In case (c), we have shown that a crossover frequency exists, proportional to the bias, (i.e., strength of the electric field) below which the real part of the conductivity diminishes as ω^2 and the imaginary part increases as ω^3. Above the crossover frequency, the real and imaginary parts increase as $\omega^{1/2}$. We have exhibited numerous graphs which show the real and imaginary parts of $\sigma(\omega)$ over the applicable frequency range.

We have limited ourselves to the first correction term for the R_n [Eq. (18)] when we work to lowest order in the disorder [case (c) above]. To that order, the frequency dependence we have found for $\sigma(\omega)$ is exact. One can pose the question of the effect on $\sigma(\omega)$ of introducing higher-order corrections in Eq. (18). Such a task is formidable, but we know the answer in the symmetric case ($a=1$). There, the $\sigma(\omega)$ can be expanded as a power series in $\langle\epsilon^n\rangle$. One finds[9] that these terms carry with them only higher powers of $\omega^{1/2}$:

$$\sigma(\omega)\propto\sigma(0)+O(\langle\epsilon^2\rangle)\omega^{1/2}+O(\langle\epsilon^3\rangle)\omega+\cdots .$$

Thus, to lowest order in $\langle\epsilon^2\rangle$, one obtains the first frequency-dependent correction to $\sigma(\omega)$, proportional to $\omega^{1/2}$. To higher order in ϵ, one obtains yet higher powers of $\omega^{1/2}$. This suggests (but we have no proof) that the next term in an expansion in the disorder for the asymmetric case would yield frequency corrections of a higher power than we have found in Sec. IV. Said another way, it may be the case that the weak-disorder limit may in fact generate only the lowest-frequency correction to the dc conductivity in the asymmetric limit (as it does in the symmetric case), with higher-frequency corrections arising from higher-order terms in the expansion in powers of the disorder (as it does in the symmetric case). This conjecture remains to be proven, but if true it means that our expressions for case (c) above can be regarded as a low-frequency expansion for the situation where the disorder is not necessarily weak.

Finally, we have shown for weak disorder that one can obtain a closed form expression for the Laplace transform of the variance of the autocorrelation function. We have succeeded in obtaining the inverse for the symmetric case, and have shown that fluctuations above the mean value fall off as $t^{-1/2}$ for long times.

ACKNOWLEDGMENTS

The authors wish to acknowledge very helpful discussions with Dr. J. Bernasconi and Dr. W. R. Schneider, and receipt of their interesting work on transport for asymmetric hopping rates prior to publication. The research of one of us (R.O.) was supported in part by the U.S. National Science Foundation and the U.S. Office of Naval Research.

*Permanent address: Department of Physics, University of California, Los Angeles, California 90024.

[1]S. Alexander, J. Bernasconi, W. R. Schneider, and R. Orbach, Rev. Mod. Phys. 53, 175 (1981).
[2]S. Alexander and R. Orbach, Physica 107B, 675 (1981).
[3]S. Alexander, J. Bernasconi, W. R. Schneider, and R. Orbach, in *Physics in One Dimension*, Vol. 23 of *Springer Series in Solid State Sciences*, edited by J. Bernasconi and T. Schneider (Springer, Berlin, 1981), p. 277.
[4]S. Alexander, J. Bernasconi, W. R. Schneider, R. Biller, W. G. Clark, G. Gruner, R. Orbach, and A. Zettl. Phys. Rev. B 24, 7474 (1981); S. Alexander, J. Bernasconi, W. R. Schneider, R. Biller, and R. Orbach, Mol. Cryst. Liq. Cryst. 85, 121 (1982).
[5]M. J. Stephen, J. Phys. C 14, L1077 (1981).
[6]B. Derrida and Y. Pomeau, Phys. Rev. Lett. 48, 627 (1982).
[7]J. Bernasconi and W. R. Schneider, J. Phys. A 15, L729 (1982).
[8]M. J. Rice, S. Strassler, and W. R. Schneider, in *One Dimensional Conductors*, edited by H. G. Schuster (Springer, Berlin, 1975), pp. 307–309.
[9]Reference 2, and J. Machta, Phys. Rev. B 24, 5260 (1981); R. Zwanzig, J. Stat. Phys. 28, 127 (1982); I. Webman and J. Klafter, Phys. Rev. B 26, 5950 (1982).

Superconducting transition temperature in anodized aluminum

C. Leemann, J. H. Elliott, G. Deutscher,* and R. Orbach
Department of Physics, University of California, Los Angeles, California 90024

S. A. Wolf
Naval Research Laboratory, Washington, D.C. 20375
(Received 2 May 1983)

We have measured the superconducting transition temperature of anodized aluminum films of grain sizes ranging from less than 100 to 3000 Å. The transition temperature is 1.8 K for films of grain size 100 Å and decreases monotonically with increasing grain size to 1.2 K for 3000-Å grains. The effect depends only on the volume of the grains.

The enhancement of the superconducting transition temperature T_c in granular aluminum has been the subject of numerous experimental investigations.[1-3] An unavoidable difficulty with the granular aluminum is that the grain size is strongly dependent on the partial oxygen pressure during evaporation, making it virtually impossible to distinguish between the effect of the reduced grain size and that of the presence of the oxide. This led us to study anodized aluminum: both effects are still present, but they are much more easily separated. We find that in our anodized aluminum films of grain sizes from ~ 100 to ~ 3000 Å, the T_c enhancement can be attributed to a variation in the grain size, in agreement with the conclusions reached by Chui *et al.*[3] for granular aluminum films. Our results indicate that the effect is independent of the surface-to-volume ratio of the grains: the only relevant parameter seems to be the grain volume. All samples reported here were fabricated by evaporation in a high vacuum and further processed with the use of photolithographic and anodization techniques. The substrates were precleaned with the use of acetone washes in an ultrasonic cleaner followed by an alcohol vapor bath. Aluminum was evaporated from an electron beam gun in a high vacuum (base pressure $\lesssim 3\times10^{-6}$ torr) onto heated sapphire substrates. Substrate temperature varied from 40 to 250 °C, resulting in a variation in grain size from 300 to 4000 Å.[4] The film thickness was measured with a crystal quartz monitor. With use of standard photolitography, the films were etched to leave samples that were $\sim 0.28\times1.22$ mm. The thicknesses of the samples were further varied with an anodization method.[5] A constant current was passed through a solution of saturated boric acid and ammonium hydroxide with the use of a platinum cathode and the aluminum sample as the anode. This converted the aluminum into oxide, resulting initially in a linear increase in the anode-cathode voltage with time. The anode-cathode voltage being essentially the voltage across the oxide, this region represents an increase of the oxide thickness, i.e., a thinning of the aluminum film at a rate of approximately 10 Å/V. At a film resistance of $50R_0$, where R_0 is the initial film resistance, the anodization voltage begins to increase at a faster rate, indicating that the film is not only getting thinner, but grains are being isolated from one another. In this manner a series of samples, with resistances from 2 to 10^4 Ω, was produced. The resistance of these samples was measured in a liquid ^{4}He cryostat by passing a constant current ($I = 10$ μA) through them and measuring the voltage drop by use of an HP3455A digital

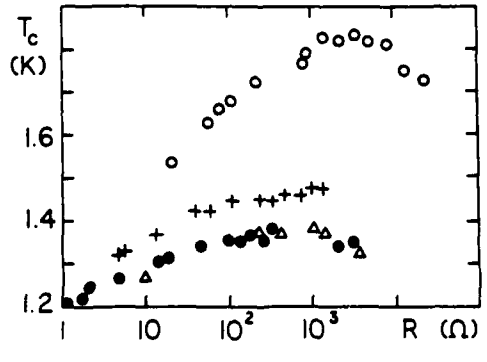

FIG. 1. Variation of T_c with sample resistance. ○, *O* series; +, *R* series; ●, *M* series; △, *P* series.

TABLE I. Properties of the unanodized samples.

Sample series	T_s (C)	d_0 (Å)	l_0 (Å)	$R_{300}/R_{4.2}$
O	40	300	230	1.3
R	115	800	500	2
M	250	4000	1000	5
P	250	4000	800	4

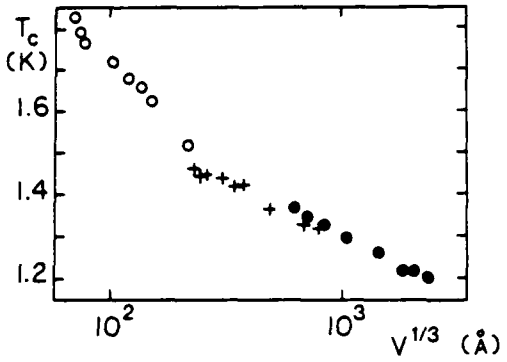

FIG. 2. Transition temperature as a function of the cube root of the grain volume. ○, *O* series; +, *R* series; ●, *M* series.

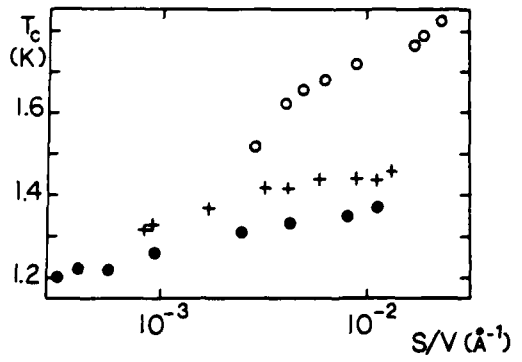

FIG. 3. Transition temperature as a function of the grains' surface-to-volume ratio. ○, *O* series; +, *R* series; ●, *M* series.

voltmeter. The temperature was monitored with a Lakeshore Cryogenics germanium resistor. The transition temperature T_c was defined to be the temperature at which the resistance falls to one-half its "normal" value above the transition.

For low normal-state resistance ($R \lesssim 100\ \Omega$) the transition width was small ($\delta T/T_c < 0.02$). At high resistances, however, this width increases and for one sample (series *O*) the transition was incomplete down to 1.17 K, the lowest temperature measured in these experiments. The variation in T_c with sample resistance is shown in Fig. 1. Four different series of samples are plotted, the parameters of which are listed in Table I.

In Table I, T_s is the substrate temperature during evaporation, t_0 is the thickness of the evaporated films, and $R_{300}/R_{4.2}$ is the residual resistance ratio of the unanodized films. The values of d_0, the grain size of thick films grown under the same conditions, are not known exactly. The values listed are inferred from the relationship between substrate temperature and grain size,[4] and are consistent with grain sizes observed in electron micrographs of similar films. The error involved is probably $\sim 30\%$.

Figure 1 shows that T_c initially increases with increasing resistance, in qualitative agreement with the measurements of Deutscher *et al.*[2] for the case of granular aluminum. At approximately $10^3\ \Omega$ (the resistance region in which anodization isolates the grains) the transition temperature levels off and then decreases for even larger resistance values. The dependence of T_c in $\log d$ for three series of samples is plotted in Fig. 2. The grain size d is defined as $d = (d_0^2 t)^{1/3}$; i.e., d is a measure of the grain volume. Only the samples with resistance values $R \lesssim 100 R_0$ are plotted, where R_0 is the resistance of the unanodized film of the series. Since for these samples d_0 is virtually unaffected by the anodization, the sample thickness t can be derived from the sample resistance at room temperature, with the corrections necessary for increased surface scattering.[6] The values of d_0 used for Fig. 2 are 200, 900, and 3500 Å for the *O*, *R*, and *M* series, respectively. These values have been chosen to improve the agreement between the three series and are well within the uncertainty of the values listed in Table I.

In the small grain size region ($d \lesssim 200$ Å), Fig. 2 agrees, within experimental error, with the measurements on granular aluminum reported in Ref. 3. For large grain sizes the slope of the T_c vs $\log d$ curve appears to increase (become less negative) and reach bulk T_c value at $d \sim 3000$ Å.

One of the models proposed to explain the increased T_c of granular aluminum films is based on an increase in the low-frequency density of states of the phonon spectrum brought about by the high surface-to-volume ratio of the grains[7] ("phonon softening"). This would require that the increase in T_c be proportional to S/V, the surface-to-volume ratio of the grains. For our grains one would expect $S/V = 4k/d_0 + 2/t$, where k, of order unity, depends on the shape of the grains. A plot of T_c vs $\log(S/V)$ is shown in Fig. 3. For any one series of samples T_c increases monotonically with S/V, in agreement with the phonon softening model. However, for every sample series the slope on the T_c vs $\log(S/V)$ graph appears to be different. We conclude that, as evidenced by Fig. 2, the T_c enhancement in anodized aluminum films is a function of the grain volume. The phonon softening model appears to break down for thin grains.

ACKNOWLEDGMENTS

This work was supported by the U.S. Office of Naval Research under Grant No. N00014-75-0245.

*Permanent address: Department of Physics and Astronomy, Tel-Aviv University, Ramat Aviv, Israel.

[1]B. Abeles, in *Applied Solid State Science: Advances in Materials and Device Research*, edited by R. Wolfe (Academic, New York, 1976), Vol. 6, p. 1.

[2]G. Deutscher, H. Fenichel, M. Gershenson, E. Grünbaum, and Z. Ovadyahu, J. Low Temp. Phys. 10, 231 (1973).

[3]T. Chui, P. Lindenfeld, W. L. McLean, and K. Mui, Phys. Rev. B 24, 6728 (1981).

[4]K. Pearman and G. Dorey, Royal Aircraft Establishment Technical Report No. 67060 (unpublished).

[5]D. W. Palmer and S. K. Decker, Rev. Sci. Instrum. 44, 1621 (1973).

[6]D. C. Larson, in *Physics of Thin Films: Advances in Research and Development*, edited by M. H. Franscombe and R. W. Hoffman (Academic, New York, 1968), Vol. 6, p. 81.

[7]W. L. McMillan, Phys. Rev. 167, 331 (1968).

Time Decay of the Remanent Magnetization in Spin-Glasses

R. V. Chamberlin, George Mozurkewich, and R. Orbach
Department of Physics, University of California, Los Angeles, California 90024
(Received 13 July 1983; revised manuscript received 1 November 1983)

The time decay of the thermoremanent magnetization (σ_{TRM}) has been measured in 1.0% Cu:Mn and 2.6% Ag:Mn spin-glasses. It is shown that σ_{TRM} is neither an algebraic nor a logarithmic function of time, but it is found that σ_{TRM} can be characterized by a "stretched" exponential: $\sigma_{TRM}=\sigma_0\exp[-C(\omega t)^{1-n}/(1-n)]$. Similar time dependences appear in the disorder-diffusion theory of Grassberger and Procaccia and the cooperative-relaxation theory of Ngai, but neither theory in its present form is directly applicable to spin-glasses.

PACS numbers: 75.30.Kz, 75.50.Kj

When measured in a small static field, the temperature dependence of the magnetization of a spin-glass changes abruptly at the glass temperature (T_g): Above T_g the magnetization obeys the Curie-Weiss law, attributable to weakly interacting paramagnetic spins, whereas below T_g the magnetization is nearly independent of temperature, indicative of the spin-glass state. The time dependence of the magnetization also changes dramatically in the vicinity of T_g: In the paramagnetic region the entire magnetization responds rapidly to a change in field, but in the spin-glass region some of the magnetization responds much more slowly.[1] One technique of investigating this viscous behavior is to apply a field (H) when the sample is in the paramagnetic region, field cool it through T_g, then remove H and measure the field-cooled remanence or "thermoremanent magnetization" (σ_{TRM}).[2]

The exact form of the time dependence of σ_{TRM} has not been previously established. Many investigators[3] have reported a logarithmic decay: $\sigma_{TRM}=\sigma_0[1-(1-n)\log(t)]$, where σ_0 and n are constants. Such a decay is unbounded, however, and must be merely an approximation, valid over some finite interval of time. The Sherrington-Kirkpatrick mean-field model[4] has been successful in describing many of the observed properties of spin-glasses. Calculations based on this model[5] suggest that the magnetization should decay algebraically: $\sigma_{TRM}=\sigma_0/t^{1-n}$. This suggestion seems plausible since for $n<1$ it approaches the correct equilibrium at long times (zero magnetization in zero field[6]), but no data have yet been published[7] supporting an algebraic decay for σ_{TRM}.

We have made magnetization measurements in the interval from 0.2 to 1000 sec after removing H and conclude that σ_{TRM} has neither an algebraic nor a logarithmic time dependence. We do, however, find that the time dependence is accurately characterized by a "stretched" exponential of the form

$$\sigma_{TRM}=\sigma_0\exp[-C(\omega t)^{1-n}/(1-n)]. \quad (1)$$

Here the exponential factor (C) and relaxation frequency (ω) can be chosen to be independent of temperature throughout the spin-glass region, whereas the prefactor (σ_0) and time-stretch exponent (n) are temperature-dependent constants.

We have made time-decay measurements on three different samples: 1.0% Cu:Mn, 2.6% Ag:Mn, and 2.6% Ag:Mn + 0.46% Sb, all of which show qualitatively similar behavior. Here we will present only the 2.6% Ag:Mn + 0.46% Sb data. Measurements were made on a stack of thin ($\sim 25\ \mu$m) foils with a total mass of 0.223 g. The glass temperature for this sample ($T_g=9.30$ K) was determined from the maximum in the magnetization in a static field of 3 Oe. We used a SQUID magnetometer to measure σ_{TRM} as follows: (1) a magnetic field ($H=30$ Oe or $H=15$ Oe) was applied to the sample when in the paramagnetic region, (2) the sample was field cooled through T_g to a temperature in the spin-glass region, (3) H was removed and the time dependence of the magnetization was recorded by a computer-based data acquisition system; (4) after 1000 sec the remaining remanence was measured by warming the sample through T_g to establish the base line.

Figure 1(a) is a plot of σ_{TRM} vs $\log(t)$ at four temperatures within the spin-glass region. The fact that the slope changes with time shows that σ_{TRM} does not decay logarithmically. Figure 1(b) is a log-log plot of the same data, here demonstrating that σ_{TRM} does not decay algebraically. In Fig. 2 we show that σ_{TRM} decays by a stretched exponential function of time. The time-stretch exponent (n) is most easily determined by plotting $\log[-(d/dt)(\ln\sigma_{TRM})]$ as a function of $\log(t)$. This is done in Fig. 2(a) where a fit to the data after 5 sec yields:

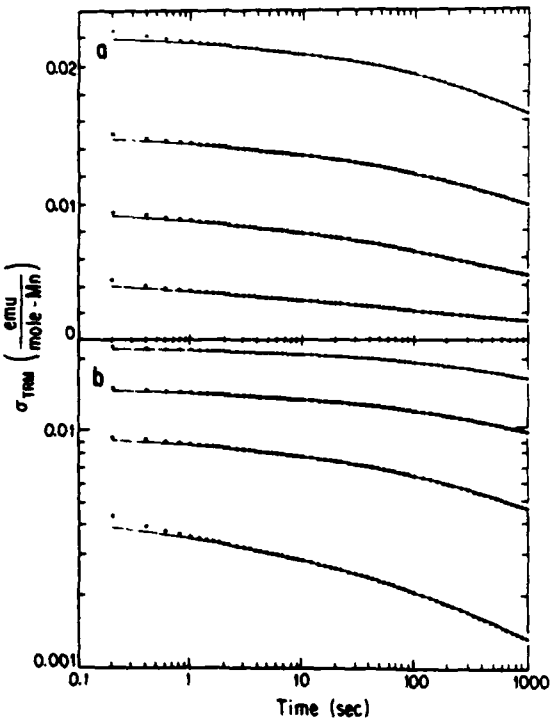

FIG. 1. (a) Semilog and (b) log-log plot of the thermoremanent magnetization (σ_{TRM}) of 2.6% Ag:Mn + 0.46% Sb as a function of time at $T/T_g = 0.771$, 0.856, 0.897, and 0.966, from top to bottom, respectively. The solid curves are the best stretched-exponential fits to the data.

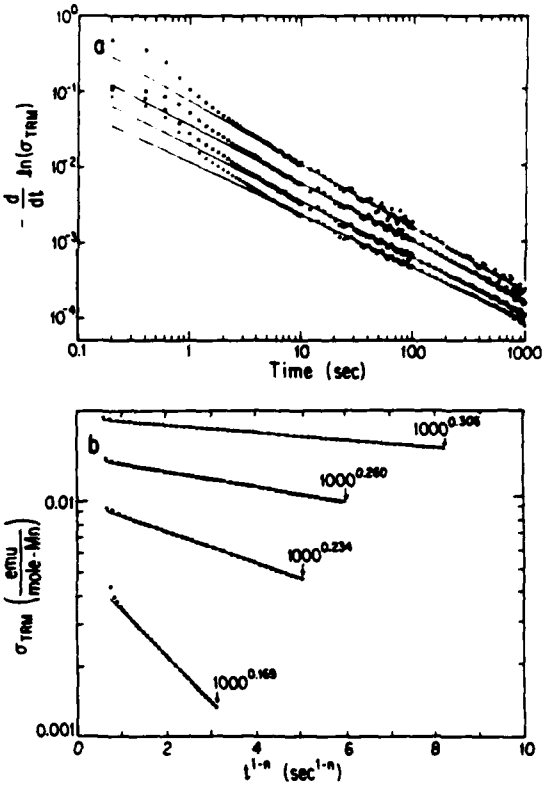

FIG. 2. Determination of the time-stretch exponent, n. (a) Log-log plot of $-d\ln(\sigma_{TRM})/dt$ as a function of time. The slope gives $-n$ and the $t = 1$-sec intercept gives $C\omega^{1-n}$. (b) Semilog plot of σ_{TRM} as a function of t^{1-n}. The solid lines are the best fits to the data.

$n = 0.694$, 0.740, 0.766, and 0.831 for $T/T_g = 0.771$, 0.856, 0.897, and 0.966, respectively. The stretched exponential nature of σ_{TRM} is verified in Fig. 2(b) by the linear dependence of $\log(\sigma_{TRM})$ on t^{1-n}. The quality of agreement is also shown in Fig. 1, where we plot the best stretched exponential fit to each set of data. The deviation before 5 sec can be attributed to the decay of induced eddy currents in the metallic samples as is evidenced by a measurable magnetic absorption,[8] even in the paramagnetic region, at frequencies above 0.2 Hz. After 5 sec, σ_{TRM} is accurately characterized with the four parameters σ_0, C, ω, and n. Note that no adjustment is allowed in the base line of the data since it is unambiguously established in step 4 of our procedure.

The temperature dependence of the prefactor and the time-stretch exponent is shown in Fig. 3. At low temperatures ($T < 0.75T_g$) σ_0 decreases linearly with increasing temperature whereas $n \simeq \frac{2}{3}$ independent of temperature. For $T > 0.75T_g$, n increases while σ_0 decreases more rapidly than at lower temperatures. The temperature dependence of n allows us to extract the relative values of ω and C by plotting $\log(C\omega^{1-n})$, obtained from Fig. 2(a), as a function of $1-n$. This is done in Fig. 4 where linear regression to the data yields $C = 0.59 \pm 0.05$ and $\omega = (3 \pm 1) \times 10^{-6}$ sec^{-1}. The only difference we measure between cooling the sample in $H = 15$ Oe and in $H = 30$ Oe is a linear dependence σ_0 on H. n, C, and ω do not depend on the cooling field for these relatively small values of H; thus, the changes in n and σ_0 for $T > 0.75T_g$ cannot be attributed to the saturation of σ_{TRM} in H.[9]

Two separate theories of relaxation, which have recently appeared in the literature, give a stretched exponential time behavior similar to that of Eq. (1). Neither theory has yet been applied to spin-glasses, so we can only point out the possibility of a connection. The first theory, due to Grassberger and Pro-

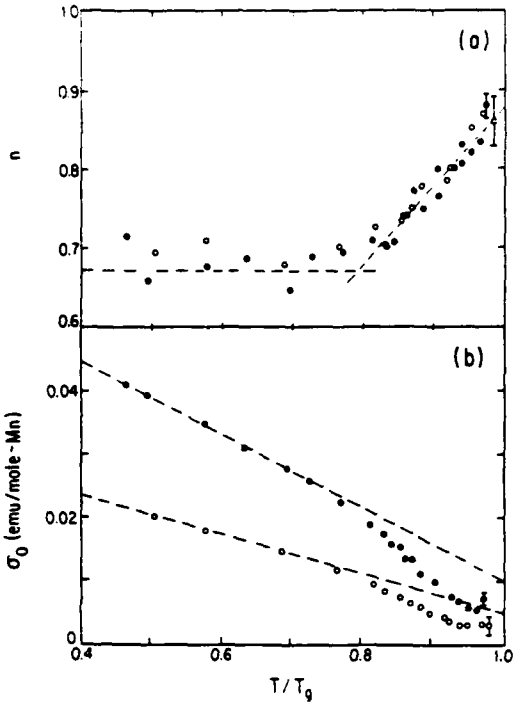

FIG. 3. (a) The temperature dependence of n. (b) The temperature dependence of the prefactor (σ_0). The solid circles are for a 30-Oe cooling field and the open circles are for $H = 15$ Oe. The dashed lines are guides for the eye.

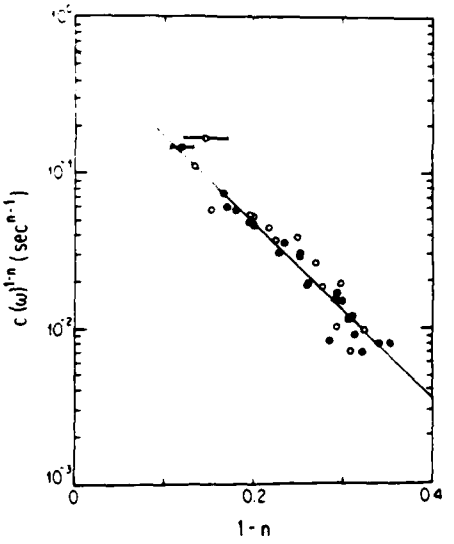

FIG. 4. Semilog plot of $C\omega^{1-n}$ as a function of $1-n$ for $H = 30$ Oe (solid circles) and $H = 15$ Oe (open circles). The solid line is the best fit to the data. The slope of this line gives $\omega = (3 \pm 1) \times 10^{-6}$ sec^{-1} and the intercept gives $C = 0.59 \pm 0.05$.

caccia,[10] considers the diffusion of particles through a d-dimensional space interspersed with randomly distributed traps. A connection to spin-glasses can be made by using the model of Bantilan and Palmer[11] in which the energy of a spin-glass is pictured as a labyrinthine function in spin-configuration space containing many maxima and local minima, and several quasidegenerate ground-state minima. The configuration of a group of spins travels randomly through configuration space until it is trapped into one of the ground-state minima. Grassberger and Procaccia find that the number of untrapped "configurations" (N_c) is given by

$$N_c \simeq f(t)\exp[-g(n)(\omega t)^{1-n}/(1-n)],$$

where the time-stretch exponent is related to the dimension of the diffusive space by $n = 1 - d/(d+2)$. Although this interpretation is interesting, three experimental facts emphasize the need for further development before this model may apply to spin-glasses. First, σ_{TRM} obeys a simple stretched exponential of time; we do not measure any time dependence to the prefactor [$f(t)$]. Second, we can choose ω so that the exponential factor [$g(n)$] is independent of n. And third, we find $n \geq \frac{2}{3}$, which implies a nonphysical ($d \leq 1$) configuration space.

The second theory giving a stretched exponential time decay is due to Ngai.[12] The Ngai theory treats the cooperative relaxation of a primary system of dipoles perturbatively coupled (coupling constant V) to a secondary continuum of low-energy excitations whose density of available levels is linear in energy: $N(E) = \alpha E$. In the Ngai model the measured susceptibility of a sample is due entirely to the particular microstate of the dipolar system, but the rate at which the dipoles approach equilibrium is influenced by the continuum. If the coupling could be ignored, the dipoles would make transitions at some time-dependent rate, $1/T_0$. But if this coupling is not negligible, the dipole transitions will excite the continuum, which in turn will influence the transition rate. Ngai gives the susceptibility as a function of time [$\phi(t)$] from which the magnetic response to the removal of H at $t = 0$ is easily found:

$$M(t) = H\int_0^t \psi(t')\,dt' = H\psi_0 \exp\left[-\left(\frac{e^{-\gamma}}{T_0 E_c^n}\right)\frac{t^{1-n}}{1-n}\right]. \quad (2)$$

where E_c is a cutoff energy for the low-energy excitations and the time-stretch exponent is given by $n = \alpha V^2$. If E_c and $1/T_0$ are set equal to ω, then Eq. (2) has the same form as Eq. (1). The Ngai theory gives a specific value for the exponential factor in terms of Euler's constant: $C = e^{-\gamma} = 0.5615\ldots$ which, to within experimental accuracy, is the value we measure. The Ngai model empirically characterizes the observed time dependence of σ_{TRM}, but a significant inconsistency still exists: Eq. (2) is an approximation supposedly valid only at long times ($E_c t >> 1$), which for $E_c = \omega \sim 10^{-5}$ sec^{-1} is never achieved in our measurements. We cannot yet explain why Eq. (2) seems to be valid throughout the time regime of our measurements. Furthermore, the source of the low-energy excitations, why $1/T_0$ should equal E_c, and the temperature dependences of σ_0 and n are not yet understood.

In conclusion, we have shown that the decay of σ_{TRM} in spin-glasses is neither a logarithmic nor an algebraic function of time. It is, however, accurately characterized at all temperatures within the spin-glass region by a stretched exponential [Eq. (1)] with four adjustable parameters. The prefactor (σ_0) and time-stretch exponent (n) are temperature dependent, whereas the exponential factor (C) and relaxation rate (ω) can be chosen to be independent of temperature throughout the spin-glass region. In addition, we find σ_0 to depend linearly on the cooling field, whereas n, C, and ω are independent of H for $H \leq 30$ Oe. We point out possible connections to two recent theories of relaxation, but emphasize that further development is necessary before either theory may be applied to the decay of σ_{TRM} in spin- glasses.

We are indebted to G. Grüner for bringing the work of Ngai to our attention. Important discussions with S. Alexander, K. L. Ngai, and L. A. Turkevich are also gratefully acknowledged. This work was supported initially by the U. S. Office of Naval Research, Contract No. N00014-75-C-0245, and subsequently by the National Science Foundation, Grant No. DMR 81-21394.

[1]R. V. Chamberlin, M. Hardiman, L. A. Turkevich, and R. Orbach, Phys. Rev. B 25, 6720 (1982).

[2]J. L. Tholence and R. Tournier, J. Phys. (Paris), Colloq. 35, C4-229 (1974).

[3]S. Oseroff, M. Mesa, M. Tovar, and R. Arce, J. Appl. Phys. 53, 2208 (1982); C. N. Guy, J. Phys. F 8, 1309 (1978).

[4]S. Kirkpatrick and D. Sherrington, Phys. Rev. B 17, 4384 (1978).

[5]H. Sompolinsky and Annette Zippelius, Phys. Rev. Lett. 47, 359 (1981).

[6]A. P. Malozemoff and Y. Imry, Phys. Rev. B 24, 489 (1981).

[7]J. Ferré, J. Rajchenbach, and H. Maletta, J. Appl. Phys. 52, 1697 (1981), find that σ_{TRM} in $Eu_{0.4}Sr_{0.6}S$ is better characterized by an algebraic decay than by a logarithmic decay, but they conclude that both forms are still only approximations.

[8]R. V. Chamberlin, M. Hardiman, G. Mozurkewich, and R. Orbach, Bull. Am. Phys. Soc. 28, 509 (1983).

[9]The data and analysis of H. Bouchiat and P. Monod, J. Magn. Magn. Mater. 30, 175 (1982), give $H_{TRM} = (2400\ \text{Oe}) \exp(-2.1 T/T_g)$ for 2.8% Ag:Mn, where H_{TRM} is a rough measure of the field above which σ_{TRM} becomes nonlinear. Thus for $T = 0.75 T_g$, $H_{TRM} \sim 500$ Oe, which supports our evidence that the change in n and σ_0 for $T > 0.75 T_g$ is not due to the saturation of σ_{TRM}.

[10]Peter Grassberger and Itamar Procaccia, J. Chem. Phys. 77, 6281 (1982).

[11]F. T. Bantilan, Jr. and R. G. Palmer, J. Phys. F 11, 261 (1981).

[12]K. L. Ngai, Comments Solid State Phys. 9, 127 (1979).

HIGH FIELD MAGNETISM
M. Date (editor)

ON THE PHYSICS OF HIGH MAGNETIC FIELDS

R. Orbach*

Ecole Supérieure de Physique et de Chimie Industrielles de la Ville de Paris
10, rue Vauquelin
75005 Paris, France

A brief list of current areas of research in high field physics is presented covering most of the presentations at this Symposium. More detailed description is given for three topics for which high magnetic fields are required, and which possess unusual interest. These are: 1) Density of states for vibrational states on fractals "Fractons", 2) Thermodynamic properties of exchange enhanced systems, and 3) p-state pairing in thin film or layered superconductors.

1. INTRODUCTION

This Symposium follows at least two others in the rapid development of high magnetic field physics.[1,2] In addition, a survey, now rather aging, of opportunities for research in high magnetic fields has been prepared.[3] The purpose of the present paper is to briefly classify the character of those papers to be presented at this Symposium, and then to describe in outline form three areas which are of particular interest to the author.

The general areas of research in high magnetic fields to be discussed at this Symposium can very roughly be titled as:
1) Collective phenomena (e.g., p-wave superconductivity)
2) Magnetic structures (e.g., phase transitions, magnetic saturation)
3) Atomic-like states (e.g., exciton structure and dynamics)
4) Diamagnetism (e.g., orientational ordering of large molecules)
5) Thermodynamic properties (e.g., field dependent susceptibilities)
6) Transport properties (e.g., quantum oscillations)
7) High energy density of states (e.g., vibrations on a fractal)

No list is complete, but this can serve as a rough outline of topics unique to high magnetic field research.

This paper will explore three of the seven areas listed above, The remaining four will be well covered by others at this Symposium. Only one of these three represents original work by this author. However, the significance of the other two warrants some attention.

Each of the three topics is described below in terms of the physical ideas which have been developed, and the possible experimental probes. Space limitations require that the reader be referred to the original treatments for the complete details.

2. DENSITY OF VIBRATIONAL STATES ON A FRACTAL, "FRACTONS"

Fractals are open, self similar structures, with interesting properties as a function of the length scale.[4] A specific example would be a percolation arrangement where the number of sites on the infinite cluster ($p > p_c$, where p_c is the percolation threshold concentration) increases not as

$$r^d$$

where r is the distance and d the Euclidean dimensionality, but rather as

$$r^{\bar{d}}$$

where $\bar{d}$ is an effective dimensionality, equal to $d - (\beta/\nu)$ in terms of the usual percolation exponents.[5] This behavior occurs for <u>short</u> length scales in comparison to the coherence length for percolation, ξ_p. For larger lengths one finds usual Euclidean[p] properties. If now one examines diffusion along the infinite cluster, the "dead ends" cause a length dependence for the diffusion constant:

$$D(r) \propto r^{-\bar{\delta}}$$

where again for percolation $\bar{\delta} = (t-\beta)/\nu$, t being the conductivity exponent.

The diffusion problem along a fractal can be solved, leading to the ensemble averaged autocorrelation function[6]

$$\langle P_0(t) \rangle \propto t^{-\bar{d}/(2+\bar{\delta})} \qquad (1)$$

where the particle has assumed to have been localized at the origin at time $t = 0$.

One now notes that the form of the diffusion equation (Master Equation) is the same as, for example, the harmonic vibrational problem, with a simple replacement of the first time derivative by the second. This mapping allows us to regard the inverse Laplace transform of Eq. (1) as the lattice vibrational density of states

(with ω^2 replacing the Laplace transform spectral parameter ϵ) for a fractal arrangement of masses and springs. One finds

$$N(\omega) \propto \omega^{\bar{p}}, \quad \bar{p} = [2\bar{d}/(2+\bar{\delta})] - 1 \quad . \tag{2}$$

For Euclidean systems, $\bar{p} = d-1$, so we are led to define, for mode counting purposes, a reciprocal space of effective dimensionality

$$\bar{d} = 2\bar{d}/(2+\bar{\delta}) \quad . \tag{3}$$

We refer to these states, when quantized, as "fractons." Their properties are most interesting. Before we outline them in more detail, some experimental examples are of interest.

Our attention to this problem was aroused by the work of Stapleton et al.[7] who measured the spin-lattice relaxation time for low-spin Fe(3+) in three hemoproteins. These large molecules were shown by x-ray measurements (counting the increase of the number of alpha carbons with distance for myoglobin at 250 K) to yield a value for $\bar{d} = 1.67 \pm 0.04$, certainly not integral. Their data for the spin-lattice relaxation time as a function of temperature for myoglobin azide (MbN_3) are copied below:

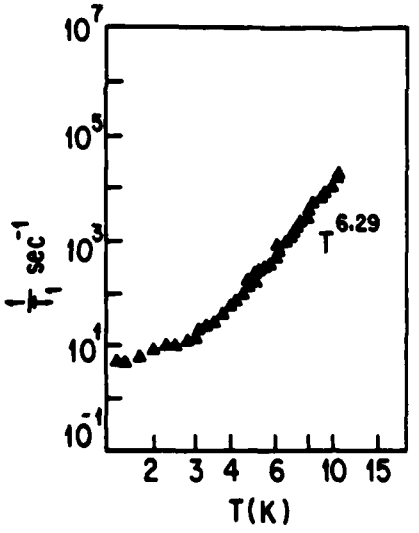

Fig. 1. The electron spin relaxation rate of low-spin Fe(3+) in MbN_3. The rate is fitted to the sum of a direction process, varying as T, and a Raman process, with temperature exponent 6.29.

Their interpretation relied on the use of the usual two-phonon integral for the Raman process relaxation rate, the integrand being proportional to the square of the vibrational density of states. Keeping all other factors the same as for Euclidean space, they extracted the exponent

$$\bar{p} = 0.65 \pm 0.04 \quad . \tag{4}$$

They did not report other data which would enable us to obtain an independent estimate for $\bar{\delta}$. The use of self avoiding random walks as a model for these proteins is inappropriate. For such systems in d = 3, [8]

$$\bar{d} = 5/3, \quad \bar{\delta} = 4/3, \tag{5}$$

leading to $\bar{d} = 1$ ($\bar{p} = 0$), representing one dimensional vibrational behavior.
The essential condition for application of these ideas to physical systems is that the length scale be less than the Euclidean correlation length. For lattice vibrations, this implies that the frequency be <u>greater</u> than a crossover frequency, $\omega_{c.o.}$, itself related to $\bar{\delta}$ by the following expression[6]:

$$\omega^2_{c.o.} \gtrsim L^{-(2+\bar{\delta})} \tag{6}$$

where L is the size of the fractal object (e.g., the percolation correlation length, or the size of the molecule) in units of the monomer length, and the frequency scale is that of the Debye frequency appropriate to the fractal object. For example, Stapleton et al. state that the temperature range 1 - 20 K is associated with wavelengths of from 10 to 10^3 bonds. For a large molecule, this would certainly be consistent with the requirement for fractal behavior.

There are other properties of fractal vibrational states. For example, the vibrational eigenfunctions are local and should not contribute to the thermal conductivity. This behavior (though not with an identification of fractal properties) has recently been reported by Kelham and Rosenberg for epoxy resin, for the energy range of 8 - 50 K (their measurements spanned the range of 0.1 - 80 K).[9]

It is clear that the identification with fractal behavior depends on the condition (6), which then leads to a vibrational density of states (2). The experimental consequences are immediate. The one phonon, or direct relaxation process rate, is directly proportional to the vibrational density of states. If one performs an electron spin lattice relaxation time measurement at sufficiently high magnetic fields, it is possible that one can obtain a direct measurement of the fracton density of states. The field must be sufficiently high that the condition (6) is satisfied. Then the field dependence of the relaxation rate will give the energy dependence of the density of fracton states, and hence a value for p using Eq. (2). The crossover magnetic field will separately give an estimate of $\bar{\delta}$ using Eq. (6). That is, $\bar{\delta}$ is not a free parameter, in that it is determined by the crossover behavior. Finally the factor $\bar{d}$ can also be determined from x-ray measurements, over-determining all the fractal parameters.

There are other interesting consequences of fractal behavior. The eigenstates are supposed to be localized. This could lead to rather interesting magnetic resonance bottleneck effects in that the spatial transfer of excitation will be diffusive rather than wavelike. This might lead to strong bottleneck conditions for both the direct and resonance relaxation processes. Here too, large magnetic fields would be useful to unravel the dynamical properties of a bottleneck. For example, if a bottleneck is found for the resonance relaxation process, the field dependence of the strength of the bottleneck will give a direct estimate of the fracton lifetime (the analysis is similar to that of Gill,[10] but using fractons instead of phonons).

3. THERMODYNAMIC PROPERTIES OF EXCHANGE ENHANCED SYSTEMS

The effect of magnetic fields upon the thermodynamic properties of Fermion systems [e.g., the nonlinear magnetic susceptibility and the field dependent specific heat], depends on the relation between field H and Fermi temperature T_F. Even for extreme fields, this ratio is small (100 Tesla is the equivalent of 170 K in Zeeman splitting). Exchange enhancement caused by electron-electron interactions in a metal can significantly enhance the effect of a magnetic field. A very recent calculation of Béal-Monod and Daniel[11] gives a complete analysis of the scaling factors in the presence of spin fluctuations (finite temperature corrections to the T = 0 results of Wohlfarth and Rhodes[12]). These can be used to obtain interesting field-induced alterations of the thermodynamics of exchange enhanced systems.

Using a method previously described,[13] the field scaling factors are found to be:

$$ST/T_F \quad , \tag{7}$$

and

$$S^{3/2}H/T_F \equiv S^{1/2}H/T_{s.f.} \quad . \tag{8}$$

Here, S is the Stoner factor,

$$S = (1 - \bar{I})^{-1}$$

where

$$\bar{I} = IN(E_F) \quad .$$

We have taken a short-range approximation for the electron-electron interaction, I, and $N(E_F)$ is the density of states at the Fermi energy. In units of the square of the magnetic moment, the Pauli susceptibility (bare) equals

$$\chi_{Pauli} = 2N(E_F) \quad .$$

We have used in Eq. (8) the usual expression for the spin-fluctuation temperature

$$T_{s.f.} = T_F/S \quad .$$

Béal-Monod and Daniel give the following expression for the magnetization of an exchange enhanced Fermi gas (parabolic band) in the temperature and field regimes $T \ll T_{s.f.}$, $H \ll T_{s.f.}/(S)^{1/2}$:

$$M(T,H) = S\,\chi_{Pauli}H\left\{1 - \alpha_1 S^2(T/T_F)^2 - \beta_0 S^3(H/T_F)^2 + (\beta_1 + 4\alpha_1\beta_0)\,S^2(T^2/T_F^2)\,S^3(H^2/T_F^2) + \cdots\right\} \quad . \tag{9}$$

Equation (9) is written in such a way that the scaling relationships are made explicit. For the parabolic band, the coefficients in Eq. (9) equal

$$\beta_0 = 1/6$$

and for H << T,

$$\alpha_1 = \pi^2/6 \quad , \quad \beta_1 = 23\,\pi^2/(24)^2$$

while for T << H,

$$\alpha_1 = \pi^2/4 \quad , \quad \beta_1 = 27\,\pi^2/(24)^2 \quad .$$

Some discussion is in order. The T = 0 value for β, β_0, is the value computed in the Stoner-Wohlfarth theory.[12] The temperature dependent contributions to M(T,H) diverge with increasing S. Fluctuations greatly enhance finite temperature corrections to M(T,H). More detailed discussions can be found in the original and complete work of Ref. 11. For more complicated bands (but still isotropic) α_1 and β_0 are known.[12,14] Béal-Monod and Daniel suggest that α_1, β_0, and β_1 will all have the same sign for arbitrary band structure.

Given Eq. (9), Béal-Monod and Daniel[11] go on to calculate the field dependence of the specific heat coefficient using a Maxwell relation. For a parabolic band they find

$$\gamma(H) - \gamma(0) = -\chi_{Pauli}\,\alpha_1\left(\frac{S^{3/2}H}{T_F}\right)^2 \times\left[1 - \left(\frac{\beta_1}{2\alpha_1} + 2\beta_0\right)\left(\frac{S^{3/2}H}{T_F}\right)^2 \cdots\right] \quad . \tag{10}$$

Béal-Monod points out[15] that the first term in Eq. (10) arises from the curvature of the zero field susceptibility at T = 0. At high fields, the second term can contribute significantly, perhaps even reversing the sign of the field dependence of γ(H), though of course higher order terms must also be included.

Comparison with experiment is becoming possible with the advent of high field measurements on exchanged enhanced materials. The case of UAl_2 will be analyzed at this Symposium by F. R. de Boer et al., and seems to show the same qualitative behavior as predicted by Eq. (9).

Béal-Monod and Daniel[11] have analyzed in some detail the case of liquid He^3 where no band structure effects are expected. At the melting pressure, S ≈ 20, and the departure from linearity of M(T,H) is predicted to be of the order of 2% at 10 Tesla. In confined geometries, however, S can be made as high as 60, giving 25% effects under the same conditions.

The case of Pd continues to be difficult to sort out. The susceptibility at H = 0 increases with increasing temperature. This implies, from Eq. (9), that α_1 is negative. This then leads one to expect an increase of the specific heat coefficient $\gamma(H)$ with increasing H using Eq. (10). This seems to be at variance with experiment, though more recent studies do seem to exhibit smaller decreases of $\gamma(H)$ with increasing H than before.[16]

The utility of Eqs. (9) and (10) lies with their relationship to one another. The two effects are not independent, and as seen in the example of Pd metal, there is a consistency requirement. One cannot simply introduce arbitrary coefficients for the temperature and field dependences of the susceptibility and specific heat. Rather, the various behaviors are linked through a set of known relationships. This should greatly assist experimental analysis, and may serve as an indication of unwanted impurities present when the consistency relations are not satisfied.

4. P-STATE PAIRING IN THIN FILM OR LAYERED SUPERCONDUCTORS

Use of high magnetic fields to achieve the p-wave condensation state for superconductors has been re-examined recently by Klemm and Scharnberg.[17] There are many problems associated with observation of this state, the most serious perhaps being that ordinary impurity scattering acts as a pair-breaker for p-wave[18] condensation, in strong contrast to the s-wave case where the Anderson theorem shows that the critical temperature is essentially unaffected. Added to this difficulty is the expectation that the p-wave transition temperature, T_T (i.e., triplet), is expected to be much smaller than T_S (i.e., singlet) for s-wave condensation. One argument favoring triplet pairing in a magnetic field is that singlet pairing (clean, type II), is limited by Pauli pair breaking,[19] but triplet pairing is not. Though this be true, Sharnberg and Klemm have recently shown[20] that orbital pair breaking in the presence of a field limits triplet condensation in nearly the same manner as for singlet condensation. As a consequence, for bulk materials, unless T_T is very close to T_S (unlikely) orbital pair breaking would prevent the upper critical field H_{c2} for triplet pairing from exceeding the Pauli $_{c2}$ limit.

The issue, then, is how to achieve a condition where orbital pair breaking can be suppressed, in the presence of large enough magnetic field to quench singlet superconductivity.

The idea of using reduced dimensionality for this purpose was first put forward by Efetov and Larkin.[21] They examined layered compounds [specifically, $TaS_2(pyridine)_{1/2}$] where a magnetic field parallel to the $^{1/2}$ layers is able to induce vortices between the metallic layers, and hence "decouple" the layers from one another. This decoupling leads to an enhancement of the upper critical field over the bulk value by (roughly)

$$\sim \ell_{tr}\, \xi_T(0)/d^2 \qquad (11)$$

where ℓ_{tr} is the transport mean free path, $\xi_T(0)$ is the zero-temperature triplet coherence length, and d the thickness of the metallic layer. This enhancement can be sufficient to exceed the Pauli limit, allowing for quenching of the singlet state. Unfortunately, this particular system has been shown to be very dirty, leading Klemm and Scharnberg to question this explanation for the observed very large $H_{c2,||}$.

In their paper,[17] Klemm and Scharnberg have analyzed the nonlocal Gor'kov gap equations for triplet pairing in the presence of magnetic fields under conditions of reduced dimensionality.

The conditions are stringent (specular surface scattering, clean thin films), but their results can conveniently be summarized by their Fig. 3:

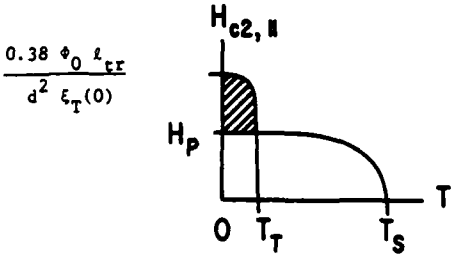

Fig. 2. Schematic plot of $H_{c2,||}(T)$ for a thin film. The shaded region is the regime of p-wave superconductivity. H_P is the Pauli limiting critical field for s-wave condensation. A similar, though more complicated, curve is exhibited by Ref. 17 for layered compounds.

Klemm and Scharnberg go on to suggest physical systems which might exhibit triplet superconductivity in high magnetic fields. They suggest cleaved thin films of $NbSe_2$, or intercalates of the same system.

One can legitimately ask, beyond the structure of Fig. 2, what signature triplet superconductivity will give which is unique to the p-wave

paired state. Buchholtz and Zwicknagl have recently pointed out that spin-polarized tunneling (pioneered by Tedrow and Meservey) in a magnetic field appears to be one of the few methods of qualitatively distinguishing its behavior from that of the singlet paired state.[22] Another difference would be the effect of magnetic proximity. Whereas a ferromagnetic layer in proximity to a singlet paired superconductor destroys the condensation over a coherence length, quite the opposite is expected to happen for triplet pairing. Indeed, it might be feasible to enhance the effect of an external field by using the proximity effect in conjunction with superposed ferromagnetic layers.

5. CONCLUSION

This paper has not attempted a general survey of the physics that can be done in high magnetic fields. Rather, it has focused on only three areas, in addition to listing those other topics which will be covered in depth by other invited speakers at this Symposium.

The author suggests that the main thrust of the three areas he has discussed are:

1) High frequency (infra-red?) electron spin resonance relaxation time measurements, as a function of frequency in the direct process regime (low temperatures, high fields), to probe the "fracton" density of states. Macromolecules, cross-linked polymers, gels, and other "open" self-similar structures would be good candidates for significant departures from the Debye density of states for lattice vibrations.

2) High magnetic field studies of magnetization and specific heat of exchange enhanced metals, to determine the thermodynamic parameters α and β. As suggested by Béal-Monod and Daniel, use of He^3 in restricted geometries may be one technique for seeing the nonlinear magnetic field properties of the Fermi gas. Another may simply be use of higher fields and lower temperatures.

3) Triplet (p-wave) superconductivity--the existence of the state and its properties. Recent work of Klemm and Scharnberg have given the limits on the magnetic field range (for clean systems, but still type-II) in which the s-wave state is quenched, but the magnetic field is below the upper critical field for p-wave pairing. The use of restricted geometry is essential in order to avoid orbital field-induced pair-breaking for the p-wave state. Thin films and layered compounds are suggested as excellent candidates.

*Permanent address: Department of Physics, University of California, Los Angeles, California 90024, U.S.A.

This research has been supported in part by the U. S. Office of Naval Research and by the U. S. National Science Foundation.

REFERENCES:

[1] Solids and Plasmas in High Magnetic Fields, Aggarwal, R.L., Freeman, A.J., and Schwartz, B.B. (eds.), (North Holland, Amsterdam, 1979).
[2] Physics in High Magnetic Fields, Chikazumi, S., and Miura, N., (eds.), (Springer-Verlag, Berlin, 1981).
[3] Opportunities for Research in High Magnetic Fields, National Academy of Sciences Study, 1980. Solid State Sciences Committee (Washington, D.C.).
[4] Mandelbrot, B.B., Fractals (Freeman, San Francisco, 1977).
[5] Kirkpatrick, S., Models of Disordered Materials, in Balian, R., Maynard, R., and Toulouse, G. (eds.), Ill-Condensed Matter (North Holland, Amsterdam, 1979), p. 321.
[6] Alexander, S. and Orbach, R., J. Physique Lettres, 1 September, 1982.
[7] Stapleton, H.J., Allen, J.P., Flynn, C.P., Stinson, D.G., and Kurtz, S.R., Phys. Rev. Lett. 45 (1980) 1456.
[8] Stauffer, D., Physics Reports 54 (1979) 1.
[9] Kelham, S. and Rosenberg, H.M., J. Phys. C: 14 (1981) 1737.
[10] Gill, J.C., J. Phys. C: 6 (1973) 109.
[11] Béal-Monod, M.T. and Daniel, E., Submitted for publication, 1982.
[12] Wohlfarth, E.P. and Rhodes, P., Phil. Mag. 7 (1962) 1817; Shimizu, M., Rep. Prog. Phys. 44 (1981) 329.
[13] Béal-Monod, M.T., Ma, S.K., and Fredkin, D.R., Phys. Rev. Lett. 20 (1968) 929; Moriya, T. and Kawabata, J., J. Phys. Soc. Japan, 34 (1973) 639.
[14] Béal-Monod, M.T. and Lawrence, J., Phys. Rev. B21 (1980) 5400.
[15] Béal-Monod, M.T., Proceedings, 16th International Conference on Low Temperature Physics, Physica, 1982.
[16] Franse, J.J.M., private communication with Béal-Monod, M.T.
[17] Klemm, R.A. and Scharnberg, K., Phys. Rev. B24 (1981) 6361.
[18] Balian, R. and Werthamer, N.R., Phys. Rev. 131 (1963) 1553.
[19] Chandrasekhar, B.S., Appl. Phys. Lett. 1 (1962) 7; Clogston, A.M., Phys. Rev. Lett. 9 (1962) 266.
[20] Scharnberg, K. and Klemm, R.A., Phys. Rev. B22 (1980) 5233.
[21] Efetov, K.B. and Larkin, A.I., Zh. Eksp. Teor. Fiz. 68 (1975) 155 [Sov. Phys.-JETP 41 (1975) 76].
[22] Buchholtz, L.J. and Zwicknagl, G., Phys. Rev. 23 (1981) 5788.